Deanship of Graduate Studies

Al-Quds University

Synthesis and Characterization of Designed Tranexamic acid prodrugs and Paracetamol prodrugs

Hiba Na`eem Khamees Ghareeb

M.Sc. Thesis

Jerusalem-Palestine

1435 / 2014

Synthesis and Characterization of Designed Tranexamic Acid and Paracetamol Prodrugs

Prepared By:

Hiba Na`eem Khamees Ghareeb

B.Sc., Pharmacy, Al-Quds University, Palestine.

Supervisor

Prof. Dr. Rafik Karaman

A thesis submitted in partial fulfillment of requirements for the degree of Master of Pharmaceutical Science, Al-Quds University.

1435/2014

Al-Quds University

Deanship of Graduate Studies

Pharmaceutical Science Program

Thesis Approval

Synthesis and Characterization of Designed Tranexamic Acid and Paracetamol Prodrugs

Prepared by: Hiba Na`eem Khamees Ghareeb

Registration No.: 21112813

Supervisor: Prof. Dr. Rafik Karaman

Master thesis Submitted and Accepted, Date: ……..

The names and signatures of the examining committee members are as follows:

1- Head of Committee: Prof. Dr. Rafik Karaman **Signature:……..**

2- Internal Examiner: Dr. Saleh Abu-Lafi **Signature:……..**

3- External Examiner: Prof. Dr. Waleed Sweileh **Signature: ……**

Jerusalem–Palestine

1435/2014

Dedication

This thesis is dedicated to my parents who sacrificed a lot for me to be what I am now. I am very grateful for their love, support and prayers.

Hiba Ghareeb

Declaration

I certify that the thesis submitted for the degree of master is the result of my own research, except where otherwise acknowledged, and that this thesis (or any part of the same) has not be submitted for a higher degree to any other university or institution.

Signed: ……..

Hiba Na`eem Khamees Ghareeb

Date: February 22, 2014

Acknowledgment

First and foremost, I am deeply thankful to Almighty **Allah** from whom I always receive help and protection.

I would like to express my special appreciation and thanks to my supervisor Professor Dr. Rafik Karaman, I would like to thank you for encouraging my research and for allowing me to grow as a researcher.

A very special thanks to Dr. Hussien halak, who has encouraged, supported me through the dark times, celebrated with me through the good, who has been a good friend and an excellent teacher.

A special thanks to my family. Words cannot express how grateful I am to my mother, father for all of the sacrifices that you've made. Your prayer for me was what sustained me thus far. I would also like to thank all of my friends who supported me in writing and gave me the incentive to strive towards my goal.

Abstract

Prodrug is a chemical devise in which the drug is covalently linked to a chemical moiety; this linked moiety will temporarily affect the physicochemical properties of the drug for increasing their usefulness or decreasing their toxicity. The prodrug should be converted to its active form by metabolic or/and chemical processes, conversion process involves metabolism by enzymes distributed throughout the body. These enzymes might either decrease the drug's bioavailability, or a genetic polymorphisms might lead to variability in prodrug activation and thus affect the efficacy and safety of designed prodrug. In the past few decades computational chemistry methods have been utilized in calculating physicochemical and molecular properties of compounds. This tool can be used to design prodrugs that chemically (intramolecular processes) interconvert to their parent drugs without any involvement of enzyme catalysis. The release of the active drug is solely dependent on the rate limiting step of the intramolecular process. Based on DFT calculations four different tranexamic acid prodrugs and three different bitter less paracetamol prodrugs were designed, synthesized and characterized using FT-IR, ^{1}H-NMR LC-MS and their in vitro intra-conversion to their parent drugs revealed that the $t_{1/2}$ was largely affected by the pH of the medium. For tranexamic acid **ProD 1** the experimental $t_{1/2}$ values in 1N HCl, buffer pH 2 and buffer pH 5 were 54 minutes, 23.9 hours and 270 hours, respectively. Tranexamic acid **ProD 2** was readily converted in 1 N HCl and pH 2 while it was entirely stable at pH 5 and pH 7.4. On the other hand, tranexamic acid **ProD 3** and **Prod 4** were stable in all media studied. The experimental $t_{1/2}$ values for paracetamol **ProD 2** in pH 3 and pH 7.4 were 3 hours and 18 minutes respectively and for paracetamol **ProD 3** it was 27 hours in pH 3 and 12 hours in pH 7.4. In vitro binding for paracetamol **ProD 2** to bitter taste receptors revealed that this prodrug lacks any binding affinity and it was found not to have any bitter sensation. This suggests, that paracetamol **ProD 2** can replace its parent drug, paracetamol, for the use as bitterless antipyretic drug for geriatrics and pediatrics.

Table of Contents

List of Tables

List of Figures

List of Abbreviations

Abbreviations	Definition
HPLC	High-performance liquid chromatography
LC-MS	Liquid chromatography-Mass spectrometry
m/z	Mass-to-Charge ratio
NMR	Nuclear magnetic resonance
ppm	Part per million
M.P	Melting point
$\mathbf{t_{1/2}}$	Half life

Introduction

Chapter one

1. Introduction

1.1. Background

The prodrug term was firstly introduced by Albert [1]. Prodrug is a chemical devise in which the drug is covalently linked to a chemical moiety; this linked moiety will temporarily affect the physicochemical properties of the drug in order to increase its usefulness or decrease its toxicity. The prodrug should be converted to its active form by metabolic or/and chemical processes. It was reported that about 10% of marketed medications are prodrugs, 20% of medicines that were approved between 2000 and 2008 were prodrugs. Therefore, nowadays the interest in prodrug approach becomes more and more popular in pharmaceutical industries [2, 3].

Ideally the prodrug should be converted to the active parent drug at the site of action; according to the site of action prodrugs can be classified into type I and type II and subtypes IA, IB, IIA, IIB or IIC. Type I are prodrugs that are converted to their parent drugs intracellularly. For subtype IA, the conversion occurs at cellular therapeutic target while in subtype IB the conversion of the prodrug occurs in metabolic tissues such as liver, but if the conversion of the prodrug occurs extracellularly, it will be classified as type II prodrug. When the conversion process occurs in gastrointestinal fluid it will be classified as subtype IIA, if the process occurs in systemic circulation or in systemic extracellular fluid the prodrug will be classified as subtype IIB, and if the conversion occurs near the target cell it will be classified as subtype IIC [4].

An ideal prodrug should have a rapid transformation to active drug when it reaches the target of interest chemically or enzymatically, and the linked moiety should be a non-toxic moiety [5].

Prodrug approach became very popular in drug development process to overcome problems related to pharmacokinetics (ADME) and toxicity which are the main factors of high attrition in drug development process so the process will be cost effective and less time consuming [6].

Applications of prodrug approach:

A. Improving solubility and bioavailability

Poor solubility of drug will be a challenge when dissolution of the drug from a dosage form is the rate limiting step. Many techniques are used to overcome solubility problem as salt formation and solubility enhancer excipients, prodrug can also be used as an alternative technique to increase aqueous solubility of parent drug by attaching polar groups such as phosphate, amino acids and sugar moieties [7-9].

If the prodrug contains a phosphate group, the parent drug will be readily released by endogenous phosphatase as alkaline phosphatase, while if it contains amino acid esters or amides the prodrug will be cleaved by esterase or amidases available in plasma or tissues, and if it contains sugar moieties such as glucose, β-glucosidase will be utilized to convert the prodrug to its corresponding parent drug [2].

B. Increasing permeability and absorption

For a drug to be absorbed, it should pass through many membranes, this requires a lipophilic group to be in the drug structure so if the drug contains polar groups it will have a limited permeability and then low absorption profile. The prodrug strategy can be used to enhance permeability by masking the polar group as hydroxyl, thiol, carboxyl, phosphate or amino acid with more lipophilic alkyl or aryl esters and these prodrugs can be readily converted to the parent drugs via hydrolysis catalyzed by esterase enzyme [10].

C. Changing distribution profile

This approach can be accomplished using a prodrug to deliver a parent drug to a specific target utilizing site- selective endogenous enzymes to convert the prodrug to its active parent drug. In addition, this approach may also be used to decrease drug toxicity [2].

D. Improving taste

If a drug has unpleasant taste, it will decrease the patient compliance and hence decreasing the efficacy of the drug. Prodrugs can be used to improve the taste of the parent drugs either by decreasing their solubility in saliva or by masking the functional group that is responsible for the binding to the taste receptors located on the tongue and thus to reducing the unpleasant taste [11].

Successfully designed prodrug should be activated to its parent drug; activation process involves metabolism by enzymes distributed throughout the body, hydrolytic enzymes as esterases and amidases and non-hydrolytic enzymes such as cytochrome P450 are the most important enzymes involved in the bioactivation process of prodrugs.

Enzymes accelerate the rate of chemical reactions that the substrate (drug) might undergo in physiological environment. The reaction rate in the majority of enzymatic reactions is 10^{10} to 10^{18} fold the non-enzymatic reaction [12].

When the prodrug is designed to be activated by natural enzymes such as esterases and amidases, the prodrug might be tackled by a premature hydrolysis during the absorption phase in enterocytes of gastrointestinal tract, this might produce more polar and less permeable prodrug which results in a decreased bioavailability (50%), while if the prodrug is activated by cytochrom P450 enzymes which are responsible for 75% of the enzymatic metabolism of prodrugs, a genetic polymorphisms might persist and then lead to variability in prodrug activation and thus affect the efficacy and safety of designed prodrugs [12]. Thus, it might be difficult to predict the bioconversion rate of the enzymatic hydrolysis of the prodrug and hence a difficulty in predicting their pharmacological or toxicological effects.

In the past few decades, computational chemistry has been utilized in calculating physicochemical and molecular properties of compounds. Using molecular orbital (MO) and molecular mechanics (MM) methods prediction of chemical reactions could be done. This tool can be used to design prodrugs that can chemically interconvert to their parent drugs without any involvement of enzyme catalysis. The release of the active drug will be

solely dependent on the rate limiting step of the intramolecular process (prodrug chemical features) [13].

1.2. Tranexamic acid

(trans-4 (aminomethyl) cyclohexanecarboxylic acid) (Figure 1.1) is a synthetic lysine derivative, it is used as antifibrinolytic to treat excessive blood loss during surgery and in other medical conditions as hemorrhage in hemophilia patients and the bleeding in tooth extraction procedure, it is a competitive inhibitor of plasminogen that prevents the activation of plasminogen to plasmin; plasmin is an enzyme used to degrade fibrin clot. It is an important agent in decreasing mortality rate due to bleeding in trauma patients; this can be seen from CRASH-2 study which concludes that all caused mortality, relative risk and relative death due to bleeding were reduced with a tranexamic acid group more than a placebo group [14]. It can be used safely in women who undergo lower segment cesarean section; in this operation it was found that tranexamic acid reduced the blood loss during and after surgery [15] , and it is pharmacologically active in reducing blood using in intra-operative heart, hip and knee replacement and liver transplant surgeries [16].

Tranexamic acid is considered as an effective medication and safe non hormonal therapy for the management of heavy blood loss during menstrual cycle and so improve women`s life quality during menses [17]. In a randomized controlled trial it was conclude that oral tranexamic acid is effective in decreasing blood loss during menstrual cycle by 40%. The total oral dose recommended in women with heavy menstrual bleeding was two 650 mg tablets three times daily for 5 days [18].

After the withdrawing of aprotinin from worldwide market at 5 November 2009, tranexamic acid is the only marketed antifibrinolytic agent available in the market [19].

It was found that tranexamic acid also is effective in inhibiting the activity of urokinase in urine [20]; so it is safe and effective to treat severe hematuria in patient with chronic renal impairment that poorly respond to conventional therapy [21].

It was found that tranexamic acid inhibit the ultraviolet radiation induced pigmentation activity hence it can be used as bleaching agents; oral tranexamic acid is effective and safe in treating malesma which is a hypermelanosis disease that occurs in Asian women

and oral tranexamic acid is a non-invasive and non-irritating treatment for this disease [22].

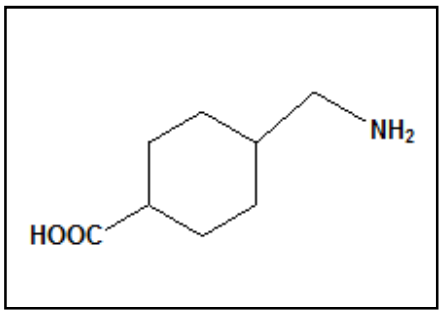

Figure 1.1. Chemical structure of tranexamic acid.

1.3. Paracetamol

Paracetamol (N-(4-hydroxyphenyl)ethanamide, Figure 1.2) is an over the counter analgesic and anti-pyretic drug. It is used to relief minor aches. it is used as pain killer by decreasing the synthesis of prostaglandin due to inhibiting cyclooxygenases [23]. Paracetamol is favored over aspirin as pain killer in patients who have excessive gastric secretion or prolonged bleeding [24]. It was approved to be used as fever reducer in all ages. Bitter unpleasant taste is one of paracetamol undesired properties.

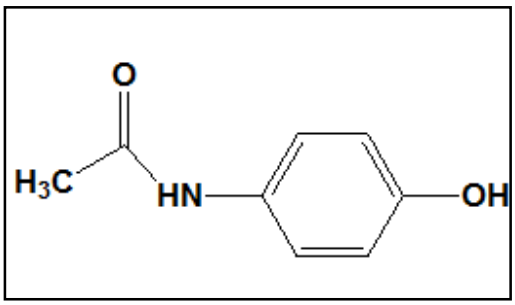

Figure 1.2. Chemical structure of paracetamol

1.3.1 Taste background

Taste is an important issue for orally administered drugs; one of the most serious problems for drug formulation is the undesirable drug's taste. Drugs bitterness might reduce patient compliance thus decreasing therapeutic effect especially in children patients. Therefore, masking the bitter taste of a drug is an important issue in the pharmaceuticals industry.

There are five basic tastes; sweet, sour, salt, bitter and umami. When a molecule dissolves in saliva it binds to a taste receptor that is found in taste buds which are distributed throughout the tongue. Sweet receptors are located on the tip of the tongue, sour receptors are located on the bilateral sides of tongue, salty taste receptors are located in the bilateral sides and the tip of the tongue, bitter taste receptors are located on the posterior part of the tongue and umami taste receptors are located all over the tongue. When a molecule binds to a receptor, a signal will be transmitted to the brain via facial, glossopharyngeal and vagus cranial nerves [25].

Human bitter taste receptors are mediated by 25 G-coupled protein receptor hTAS2Rs [26]. Binding of a bitter taste molecule to a bitter taste receptor causes an activation of a G-coupled protein receptor which leads to split α, β, γ sub units, and then a second messenger is activated leading to an increase in Ca^{+2} concentration inside the cell, thus causing a depolarization of a neuron to produce a signal which is transferred and interpreted in the brain as bitter taste [27].

1.4. Research problem

1.4.1 Tranexamic acid

Due to the amino acid nature of tranexamic acid, it can be concluded that tranexamic acid has a low bioavailability because at physiological pH it will be in an ionized form; this ionization will decrease the ability of tranexamic acid to be transferred to the systemic blood circulation and hence only 34% of tranexamic acid will be available in the systemic circulation [28].

Thus, using the prodrug approach to increase tranexamic acid bioavailability can be utilized. This can be achieved by making a covalent linkage between tranexamic acid and a non-toxic promoiety that increases the lipophilicity of tranexamic acid.

The proposed prodrug was designed using computational methods such that the prodrug will be intraconverted to tranexamic acid and non-toxic moiety in a rate which is only dependent on the structural features of the inactive linker.

1.4.2. Paracetamol

Paracetamol has a strong bitter taste (Figure 1.3). The bitter unpleasant taste of a drug might reduce patient compliance. Paracetamol was found in the urine of patients who had taken phenacetin and later on, it was demonstrated that paracetamol was a urinary metabolite of acetanilide (Figure 1.3). Phenacetin (Figure 1.3), on the other hand, lacks or has a very slight bitter taste. Examination of the structures of paracetamol and phenacetin reveals that the only difference in the structural features is the nature of the group in the *para* position of the benzene ring. While in the case of paracetamol the group is hydroxy, in phenacetin it is ethoxy. Acetanilide has a chemical structure similar to that of paracetamol and phenacetin but lacks the group in the *para* position of the benzene ring, making it lack the bitter taste characteristic of paracetamol. These combined facts suggest that the presence of a hydroxy group on the *para* position is the major contributor for the bitter taste of paracetamol. Therefore, it is expected that blocking the hydroxyl group in paracetamol with a suitable linker could inhibit the interaction of paracetamol with its bitter taste receptors and mask its bitter taste [29].

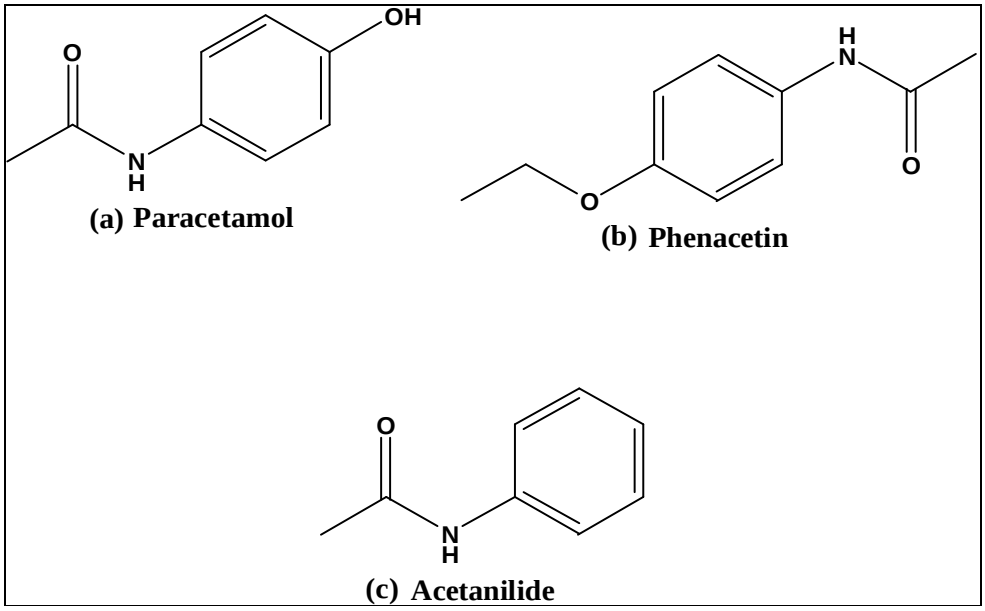

Figure 1.3 . Chemical structures of (a) paracetamol, (b) phenacetin and (c) acetanilide.

1.5. Thesis objectives

General Objective:

The main goal of this research was to synthesize and to study the kinetics for the following novel prodrugs: tranexamic acid maleate, tranexamic acid dimethyl maleate, tranexamic acid succinate, tranexamic acid dimethyl succinate, paracetamol maleate, paracetamol succinate and paracetamol glutarate.

Specific objectives:

1. To synthesize tranexamic acid prodrugs with the following characteristics:

✓ To be readily dissolved in physiological media.

✓ To increase the bioavailability profile.

✓ To have moderate hydrophilic lipophilic balance (HLB) value.

✓ To be converted to tranexamic acid in a programmable manner.

✓ To give a safe non-toxic linker moiety after conversion process.

2. To synthesize paracetamol prodrugs with following characteristics:

✓ Lack bitter taste.

- ✓ To give safe non-toxic linker moiety after conversion process.

3. To perform in vitro Kinetic studies of tranexamic acid prodrugs and paracetamol prodrugs at different pHs mimicking the physiological media.

Literature Review

Chapter Two

2. Literature Review

2.1. Introduction

Nowadays, quantum mechanics (QM) such as *ab* initio, semi-empirical and density functional theory (DFT) and molecular mechanics (MM) are recommended to provide structure energy calculations for prediction of drugs and prodrugs alike [30-34].

The *a*b initio molecular orbital methods are based on rigorous use of Schrodinger equation with number of approximations. *Ab* initio methods can be applied only on small system containing not more than thirty atoms. Semi-empirical method is applied on molecules with more than 50 atoms and gives information for practical application [35, 36]. DFT method is a semi-empirical method used for medium sized systems and it's not restricted to the second row of the periodic table [37].

The mechanisms of some intramolecular processes that were advocated to understand enzyme catalysis (enzyme models) were investigated to design novel prodrug linkers [29, 38-56]. Among the studied intramolecular processes:

- Acid-catalyzed lactonization of hydroxy-acids as researched by Cohen [30, 57, 58] and Menger [59-65].
- S_N2-based ring closing reactions as studied by Brown, Bruice, and Mandolini [31, 32, 66].
- Proton transfer between two oxygens in Kirby's acetals [67-71], and proton transfer between nitrogen and oxygen in Kirby's enzyme models [67-71], proton transfer from oxygen to carbon in some of Kirby's enol ethers [67-71].

The computational calculations using DFT and *ab* initio methods carried by Karaman's group revealed the followings: (i) rates acceleration in intramolecular processes is a result of both entropy and enthalpy effects. In intramolecular ring-closing reactions where enthalpic effects were predominant, steric effects were the determining factor for the acceleration, whereas proximity orientation was the determining factor in proton-transfer reactions. (ii) The distance between the two reacting centers is the main factor in

determining whether the reaction type is intermolecular or intramolecular. When the distance exceeded 3 Å, an intermolecular engagement was preferred because of the engagement with a water molecule (solvent). When the distance between the electrophile and nucleophile was < 3 Å, an intramolecular reaction was dominant [38-55, 72].

Based on previous studies on enzyme models a design of a prodrug with modified pharmacokinetics properties that can releases the parent drug in a slow or fast manner could be accomplished [6].

2.2. Design of Tranexamic acid prodrug using Kirby`s enzyme model (Proton transfer in N-alkylmaleamic acids)

Acid-catalyzed hydrolysis of N-alkylmaleamic acids **1-9** (Figure 2.1) was kinetically studied by Kirby's group; they concluded that the amide bond cleavage occurs due to intramolecular nucleophilic catalysis by the adjacent carboxylic acid group and the rate-limiting step is the tetrahedral intermediate breakdown [73].

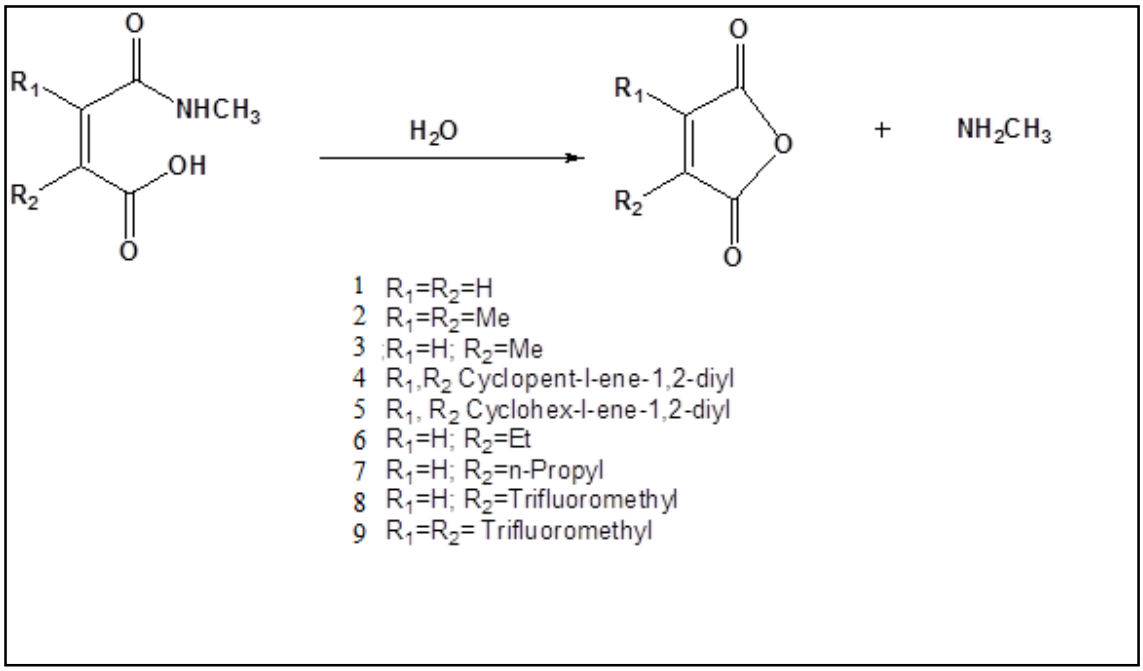

Figure 2.1. Acid-catalyzed hydrolysis of N-alkylmaleamic acids.

DFT calculations on the acid-catalyzed hydrolysis of Kirby`s N-alkylmaleamic acids that were done by Karaman's group showed that the rate limiting step in aqueous medium is

the collapse of the tetrahedral intermediate whereas in the gas phase the rate limiting step is the formation of the tetrahedral intermediate. Furthermore, Karaman's calculations revealed a correlation between the acid-catalyzed hydrolysis efficiency and the following parameters:

1. The difference between the strain energies of intermediate and product and intermediate and reactant.
2. The distance between the hydroxyl oxygen of the carboxylic group and the amide carbonyl carbon.
3. The attack angle.

The calculations also demonstrated that the acid catalyzed reaction involves three steps: (1) proton transfer from the carboxylic group to the adjacent amide carbonyl oxygen, (2) nucleophilic attack of the carboxylate anion onto the protonated carbonyl carbon; and (3) dissociation of the tetrahedral intermediate to provide products (Figure 2.2).

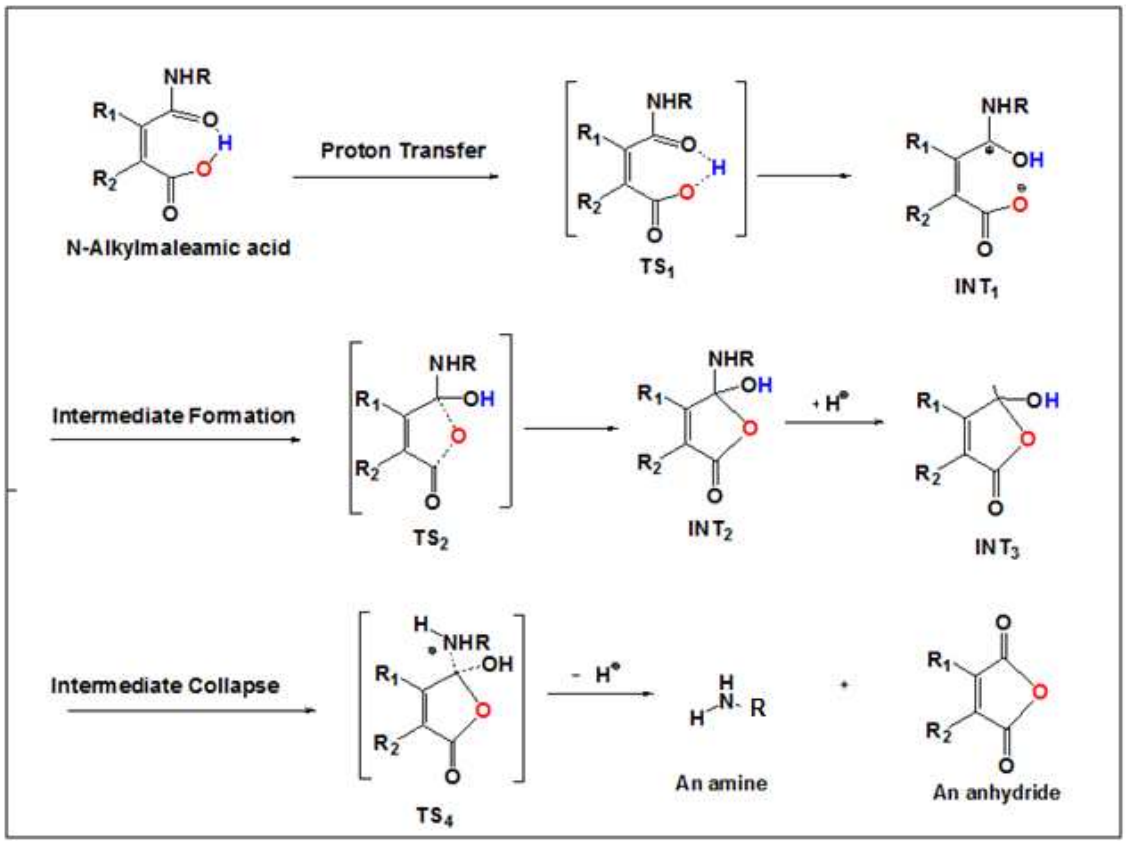

Figure 2.2. Proposed mechanism for the acid-catalyzed hydrolysis of N-alkylmaleamic acids.

Based on the calculation results of Kirby`s model (proton transfer in N-alkylmaleamic acids) we propose four tranexamic acid prodrugs, tranexamic acid **ProD 1- 4** (Figure 2.3).

As shown in Figure 6, tranexamic acid **ProD 1- 4** have a carboxylic group (hydrophilic moiety) and a lipophilic moiety (the rest of the prodrug), where the combination of both moieties secures a relatively moderate HLB.

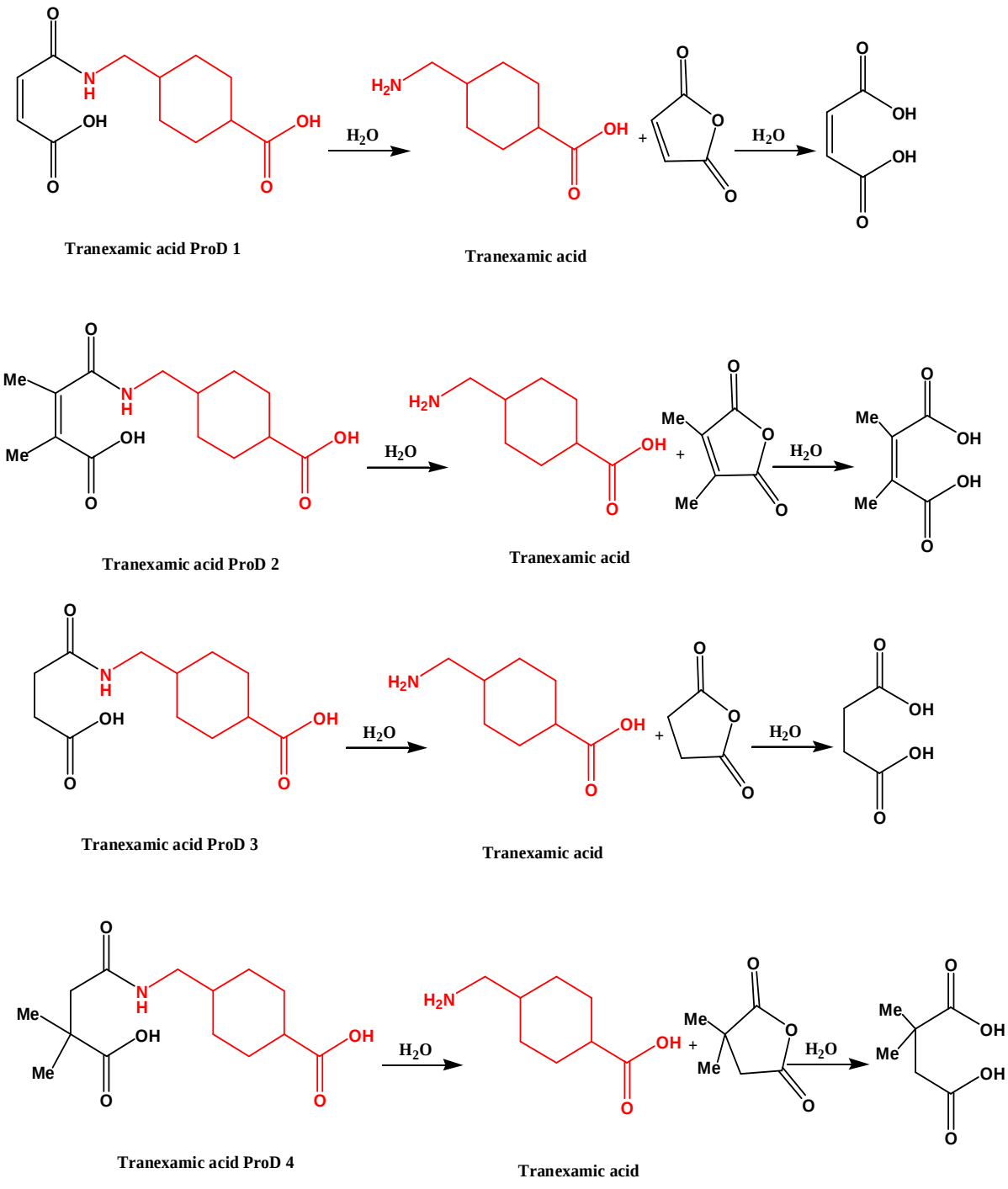

Figure 2.3. Acid-catalyzed hydrolysis of tranexamic acid **ProD 1- 4**.

In most of the physiologic environments (pH 1- 8.0) tranexamic acid will exist primary in the ionized forms (eq.1) while its prodrugs, tranexamic acid **ProD 1- 4**, will equilibrate between the ionic and the free acid forms (eq. 2) especially in a physiological environment of pH 5.5-6.8 (intestine). Thus, it is expected that tranexamic acid **ProD 1-4** may have a better bioavailability than the parent drug due to neutralizing the ionized amine group which results in absorption improvement. In addition, these prodrugs may be used in different dosage forms (i.e. enteric coated tablets, topical use and etc.) because of their potential solubility in organic and aqueous media due to the ability of the carboxylic group to be converted to the corresponding carboxylate anion in a physiological pH of around 6.0.

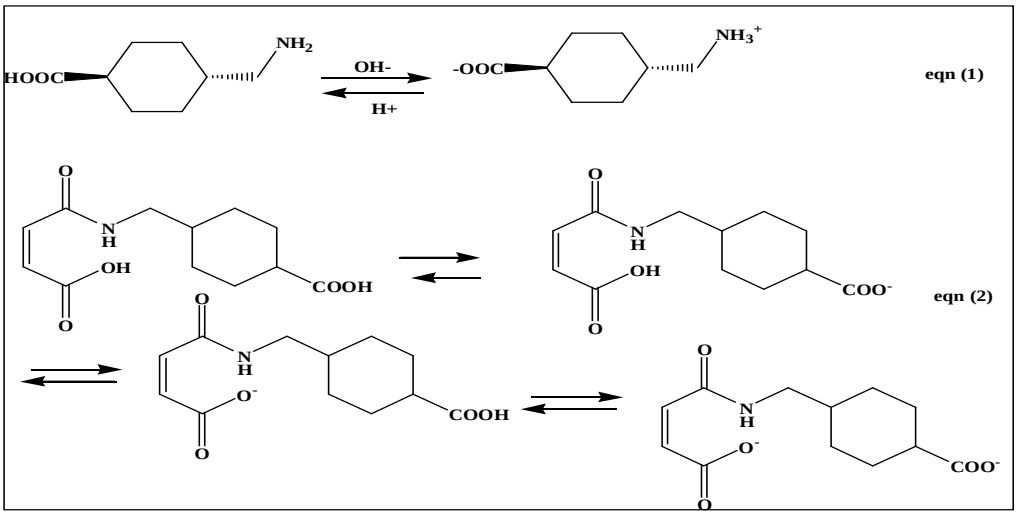

It should be emphasized that at pH 5.5-6.5 (SC, skin, mouth cavity and intestine physiologic environments), the carboxylic group of the prodrugs will equilibrate with the corresponding carboxylate form (eq. 2). Subsequently, the free acid form will undergo proton transfer reaction (rate limiting step) to yield the antifibrinolytic drug, tranexamic acid, and the inactive linker as a by-product (Figure 6).

It is worth noting that our proposal is to exploit tranexamic acid prodrugs **ProD 1- 4** for oral use via enteric coated tablets. At this physiologic environment, these prodrugs will exist in the acidic and ionic forms where the equilibrium constant for the exchange between the two forms is dependent on the pK_a of the given prodrug (eq. 2). The

experimental determined pK_{a1} for tranexamic acid **ProD 1- 4** linkers is in the range of 4-6. Therefore, it is expected that the pK_as of the corresponding prodrugs will have similar pK_a range as for the carboxylic linkers. Since the pH for the small intestine lies in the range of 5.5-6.8, the calculated unionized (acidic) /ionized ratio will be in the range of 10-50%. Although the percentage of the acidic form is not significantly high, we expect that these prodrugs to undergo an efficient proton transfer (rate limiting step) to yield the antifibrinolytic drug, tranexamic acid. In the blood circulation at pH 7.4, the calculated acidic form is around 1% and it is expected that the efficiency for delivering the parent drug will be relatively low. Improving the efficiency could be achieved by using carboxylic linkers having pK_a close to that of the blood circulation (pH 7.4).

2.3. Designing of paracetamol prodrug based on Bruice's enzyme model

Bruice's group researched the ring-closing reactions of di-carboxylic semi-esters **10**-**14** shown in Figure 2.4 and they found that the relative rate (k_{rel}) is in the following order **14** > **13** > **12** > **11** > **10**. They attributed the acceleration in rates to proximity orientation. Using the observation that alkyl substitution on succinic acid influences rotamer distributions, the ratio between the reactive gauche and the unreactive anti-conformations, they proposed that *gem*-dialkyl substitution increased the probability of the resultant rotamer adopting the more reactive conformation. Hence, for ring-closing to occur, the two reacting centers must be in the gauche conformation. In the unsubstituted reactant, the reactive centers are almost completely in the anti-conformation in order to minimize steric interactions [31, 32]

Menger and Bruice ascribed the phenomenon of rate enhancement in some intramolecular processes to the importance of the orientation (proximity) of the nucleophile to the electrophile of the ground state molecules [31, 32, 60, 62, 63]. Menger in his "spatiotemporal" hypothesis developed an equation relating activation energy to distance and based on this equation, he has reached to the conclusion that significant rate accelerations in reactions catalyzed by enzymes are obtained by imposing short distances between the reacting centers of the substrate and enzyme [62, 63]. On the other hand, Bruice attributed the enzyme catalysis to favorable 'near attack conformations'.

According to Bruice's hypothesis, systems having a high quota of near attack conformers will have a higher intramolecular reaction rate and *vice versa*. Bruice's idea invokes a combination of distance between the two reacting centers and angle of attack by which the nucleophile approaches the electrophile [31, 32]. In contrast to the proximity proposal, others believe that high rate acceleration in intramolecular processes is a result of steric effects (relief of the reactant's strain energy) [74].

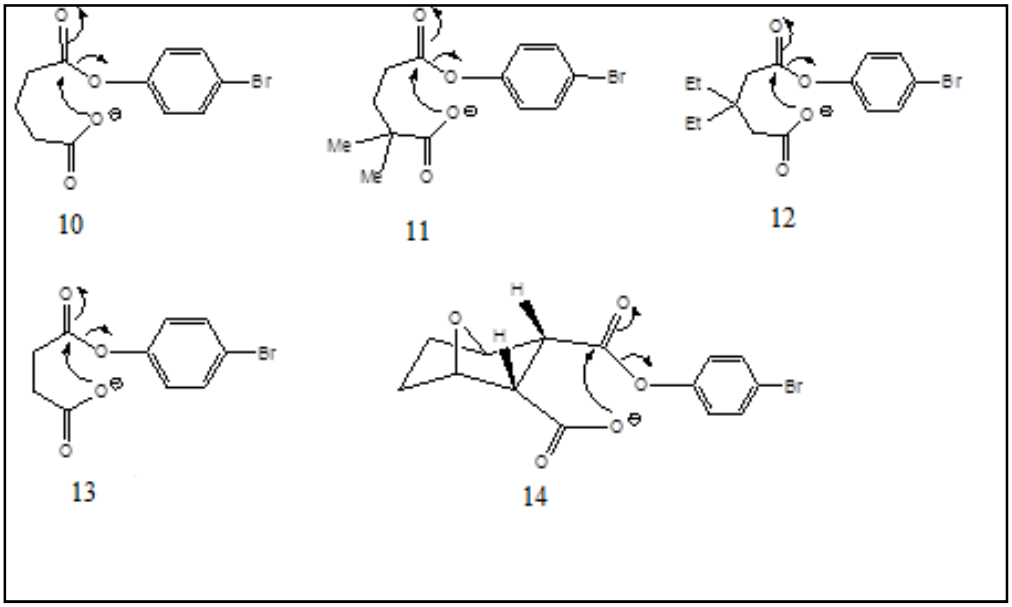

Figure 2.4. Chemical structures for di-carboxylic semi-esters **10-14**.

Reevaluation of Bruice`s proximity orientation

For utilizing di-carboxylic semi-esters **10-14** (Figure 2.4) as prodrug moieties for drugs containing hydroxyl or phenol group, Karaman's group have recently unraveled the mechanism for their ring-closing reactions using DFT and molecular mechanics (MM2) calculation methods (Figure 2.4) [72] . In accordance with the findings by Bruice and Pandit [31, 32], Karaman's study revealed that the ring-closing reaction occurs by one mechanism (Figure 2.5), by which the rate-limiting step is the tetrahedral intermediate collapse and not its formation. However, contrarily to the conclusion by Bruice, Karaman found that the acceleration in rates is due to steric effects rather than to proximity orientation stemming from the "rotamer effect" [72].

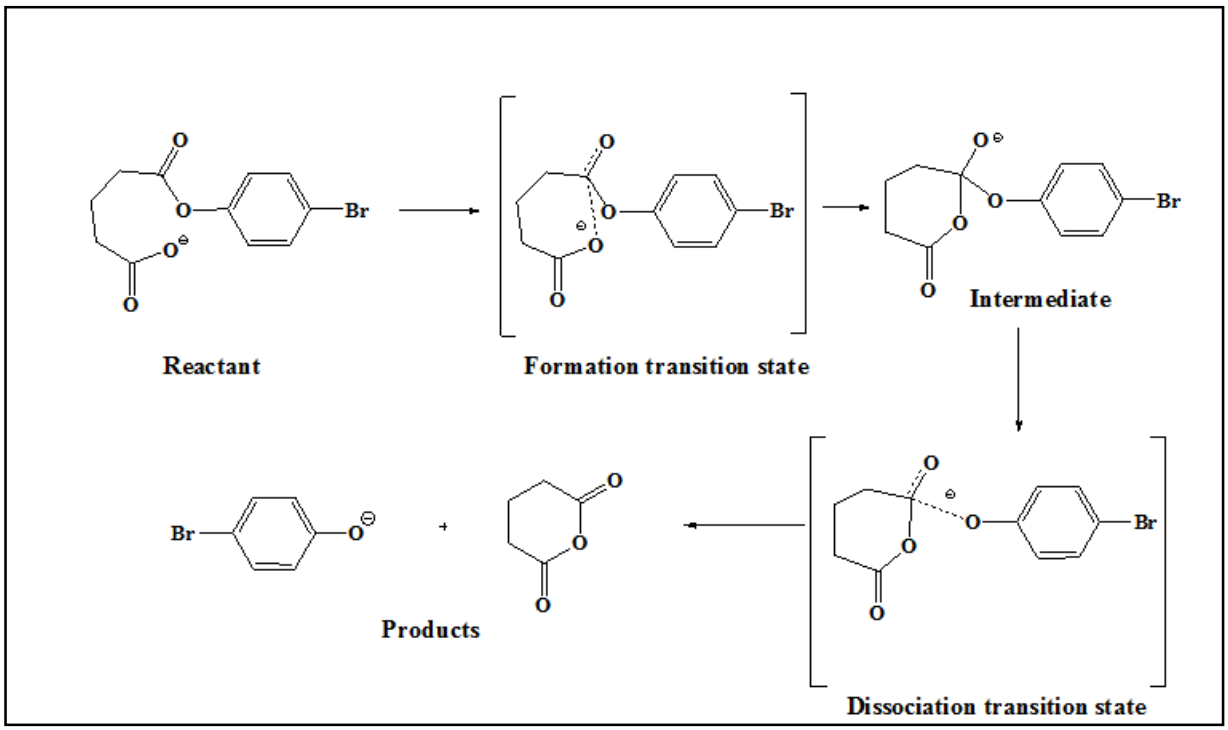

Figure 2.5. Proposed mechanism for the hydrolysis of di-carboxylic semi-esters.

Based on the calculations study of Bruice's enzyme model, we propose three paracetamol prodrugs, paracetamol prodrugs **ProD 1- ProD 3** as shown in (Figure 2.6) have a carboxylic acid group as a hydrophilic moiety and the rest of the prodrug as a lipophilic moiety, where the combination of both groups provides a moderate HLB. It should be noted that the HLB value will be determined upon the physiologic environment by which the prodrug is dissolved. For example, in the stomach, paracetamol prodrugs will primarily exist in the carboxylic acid form whereas in the blood circulation the carboxylate anion form will be predominant. Since Bruice's cyclization reaction occurs in basic medium paracetamol **ProD 1-ProD 3** were obtained as carboxylic free acid form, since this form is expected to be stable in acidic medium such as the stomach.

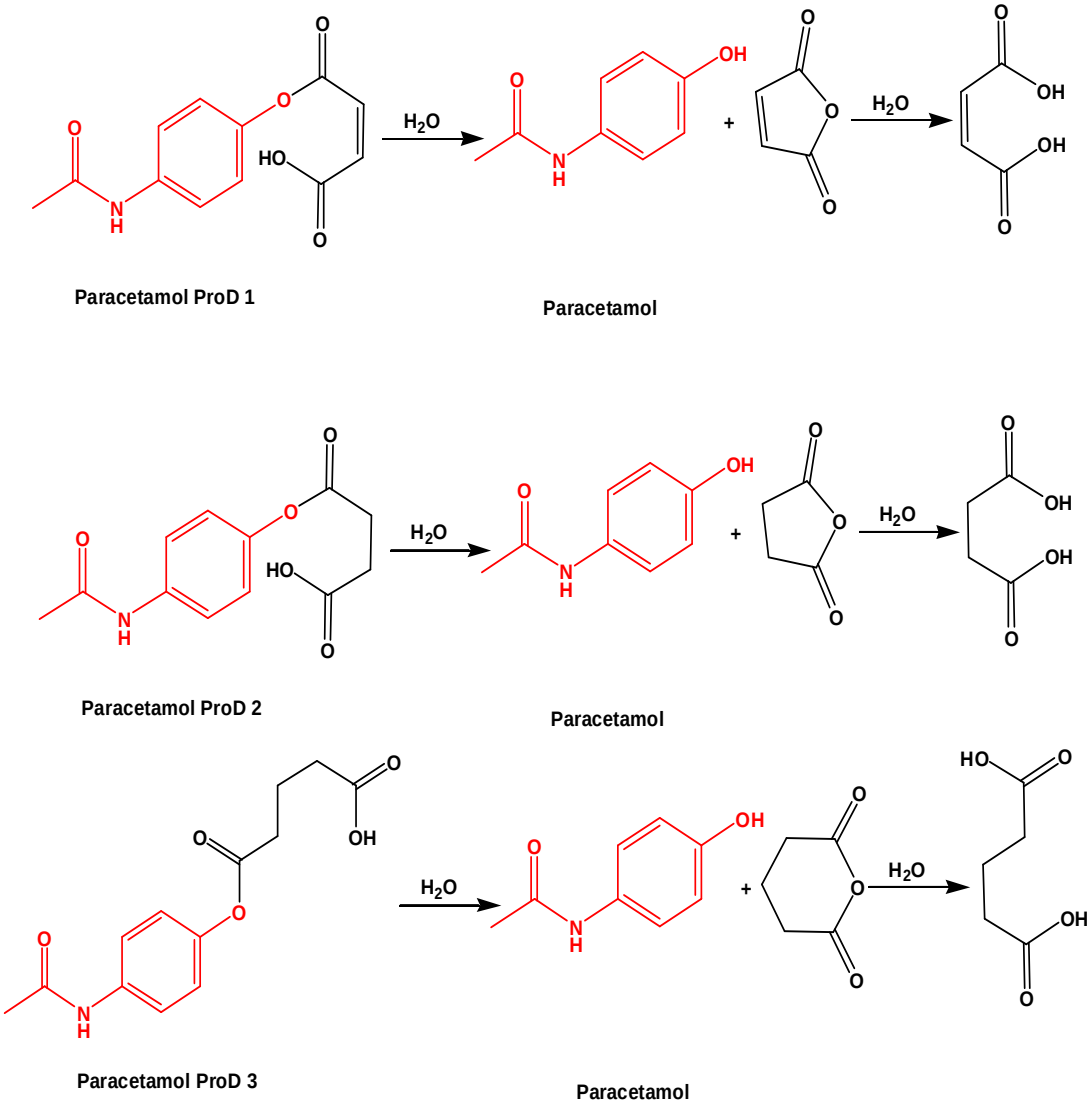

Figure2.6. Hydrolysis of Paracetamol **ProD 1- ProD 3**.

Experimental

Chapter Three

3. Experimental Part

3.1. Materials

Inorganic salts were of analytical grade and were used without further purification. Distilled water was redistilled twice before use. Maleic anhydride, succinic anhydride, 2,3-dimethyl maleic anhydride, 2,2-dimethyl succinic anhydride, sodium hydride, anhydrous sodium dihydrogen phosphate, sodium lauryl sulfate, triethylamine, tranexamic acid and paracetamol were commercially obtained from sigma Aldrich. Methanol, acetonitrile and water for analysis were for HPLC grade and were purchased from Sigma Aldrich. High purity chloroform, tetrahydrfuran (THF) and diethyl ether (> 99%) were purchased from Biolab (Israel).

3.2. Instrumentation

HPLC measurements were carried out using Shimadzu prominence high performance liquid chromatography system HPLC-PDA, (Shimadzu corp. Japan). Samples were shaken using Big Bill, (Banstaed/ Themolyne, USA). LC-Esi-MS measurements were performed employing an agilent 1200 series liquid chromatography coupled with a 6520 accurate mass quadruple time of flight mass spectrometer (Q-TOF LC/MS)The high pressure liquid chromatography system consisted of a model 2695 HPLC from Waters (Israel) equipped with a Waters 2996 Photodiode array. Data acquisition and control were carried out using Empower ™ software (Waters: Israel). Analytes were separated on a 4.6 mm x150 mm C18 XBridge® column (5 µm particle size) used in conjunction with a 4.6 mm, 20 µm, XBridge® C18 guard column. Microfilters 0.45µm porosity were normally used (Acrodisc® GHP, Waters). pH meter model HM-30G: TOA electronics™ was used in this study to measure the pH value for the buffers. UV-Spectrophotometer the concentrations of samples were determined spectrophotometrically (UV-spectrophotometer, Model: UV-1601, Shimadzu, Japan) by monitoring the absorbance at λ_{max} for each drug. Centrifuge: Labofuge®200 Centrifuge was used, 230 V 50/60 Hz. CAT. No. 284811. Made in Germany. ^{1}H-NMR: Data were collected using Varian Unity Inova 500 MHz spectrometer equipped with a 5-mm switchable and data were processed

using the VNMR software. For ^{1}H-NMR, chemical shifts are reported in parts per million (ppm, δ) downfield from tetramethylsilane (TMS). Spin multiplicities are described as s (singlet), brs (broad singlet), t (triplet), q (quartet), and m (multiplet). All infrared spectra (FTIR) were obtained from a KBr matrix (4000–400 cm^{-1}) using a PerkinElmer Precisely, Spectrum 100, FT-IR spectrometer.

3.3. Synthesis of the Prodrugs

3.3.1 *Tranexamic acid prodrugs (Scheme 1)*

In a 250 ml round-bottom flask tranexamic acid (10 mmol) was dissolved in THF (100 ml), a solution of 0.5 g NaOH in dry THF was added (50 ml), the resulting solution was stirred for 30 minutes, then 10 mmol of maleic anhydride, 2,3-dimethyl maleic anhydride, succinic anhydride or 2,2-dimethyl succinic anhydride was slowly added to the reaction mixture and stirred at room temperature for 10 hours, then the reaction mixture was refluxed for two hours and cooled to room temperature, the white precipitate formed was collected and dried.

Reaction of tranexamic acid with maleic anhydride 2,3-dimethyl maleic anhydride, succinic anhydride or 2,2-dimethyl succinic anhydride provided tranexamic acid **ProD 1, ProD 2, ProD 3** and **ProD 4** respectively with yields of 87% (2.2g), 92% (2.5 g), 92% (2.3 g) and 86% (2.4 g) respectively. M.P. 201 C^{o}, 240 C^{o}, 220 C^{o} and 215 C^{o} respectively.

Tranexamic acid **ProD 1,** ^{1}H-NMR δ (ppm) CD_3OD- 1.06 (q, 2H, CH-$\underline{CH_2}$-CH_2), 1.40 (q, 2H, CH-$\underline{CH_2}$-CH_2), 1.54 (m, 1H, CH_2-$\underline{CH}$-CH_2-CH_2), 1.84 (m, 2H, CH_2-$\underline{CH_2}$-CH), 2.02 (m, 2H, CH_2-$\underline{CH_2}$-CH), 2.22 (m, 1H, CH_2-$\underline{CH}$-CH_2-CH_2), 3.17 (d, 2H, J = 6.5 Hz, $\underline{CH_2}$-N), 6.25 (d, 1H, J = 14 Hz, HC=$\underline{CH}$), 6.45 (d, 1H, J = 14 Hz, $\underline{HC}$=CH). IR (KBr/ν_{max} cm^{-1}) 1712 (C=O), 1643 (C=O), 1587 (C=C), 1420, 1280, 1200, 1132, 1058. *m*/*z* 256.1179 $(M+1)^{+}$.

Tranexamic acid **ProD 2,** ^{1}H-NMR δ (ppm) D_2O- 1.40 (m, 1H, CH_2-$\underline{CH}$-CH_2), 1.65 (m, 4H, CH-$\underline{CH_2}$-CH_2-CH-CH_2-$\underline{CH_2}$), 1.73 (m, 2H, CH2-$\underline{CH2}$-CH), 1.93 (s,6H, $\underline{CH_3}$-C=C-$\underline{CH_3}$), 2.02 (m, 2H, CH2-$\underline{CH2}$-CH), 2.22 (m, 1H, CH2-$\underline{CH}$-CH2-CH2), 3.02 (d, 2H, J = 7.2 Hz, $\underline{CH2}$-N). IR (KBr/ν_{max} cm^{-1}) 1751 (C=O), 1646 (C=O), 1544 (C=C), 1444, 1257, 1204, 1111, 1012. *m*/*z* 566.2905 $(2M+1)^{+}$.

Tranexamic acid **ProD 3**, ^{1}H-NMR δ (ppm) CD_3OD- 0.97 (m, 1H, CH_2-$\underline{CH}$-CH_2), 1.41 (m, 4H, CH-$\underline{CH_2}$-CH_2-CH-CH_2-$\underline{CH_2}$), 1.82 (m, 2H, CH_2-$\underline{CH_2}$-CH), 1.97 (m, 2H, CH_2-$\underline{CH_2}$-CH), 2.13 (m, 1H, CH_2-$\underline{CH}$-CH_2-CH_2), 2.44 (t, J = 4.8 Hz, 2H,CH_2-$\underline{CH_2}$), 2.5 (t, 2H, J = 4 Hz, C$\underline{H_2}$-CH_2), 3.02 (d, 2H, J = 6.8 Hz, $\underline{CH_2}$-N). IR (KBr/ν_{max} cm^{-1}) 1742 (C=O), 1703 (C=O), 1642 (C=O), 1555, 1383, 1320, 1287, 1240, 1127. *m*/*z* 507.3454 $(2M+1)^{+}$.

Tranexamic acid **ProD 4**. ^{1}H-NMR δ (ppm) CD_3OD- 0.97 (m, 1H, CH_2-$\underline{CH}$-CH_2), 1.21(s, 6H, J = 20 Hz, $(\underline{CH_3})_2$-C) 1.41 (m, 4H, J = 7 Hz, CH_2-$\underline{CH_2}$-CH-$\underline{CH_2}$-CH_2), 1.82 (m, 2H, CH_2-$\underline{CH_2}$-CH), 1.97 (m, 2H, CH_2-$\underline{CH_2}$-CH), 2.13 (m, 1H, CH_2-$\underline{CH}$-CH_2-CH_2), 2.51 (s, N-C=O$\underline{CH_2}$-C) 3.01 (d, 2H, J = 6.5 Hz, $\underline{CH_2}$-N). IR (KBr/ν_{max} cm^{-1}) 1750 (C=O) 1645 (C=O), 1566, 1472, 1372, 1254, 1113, 1015. *m*/*z* 286.1627 $(M+1)^{+}$.

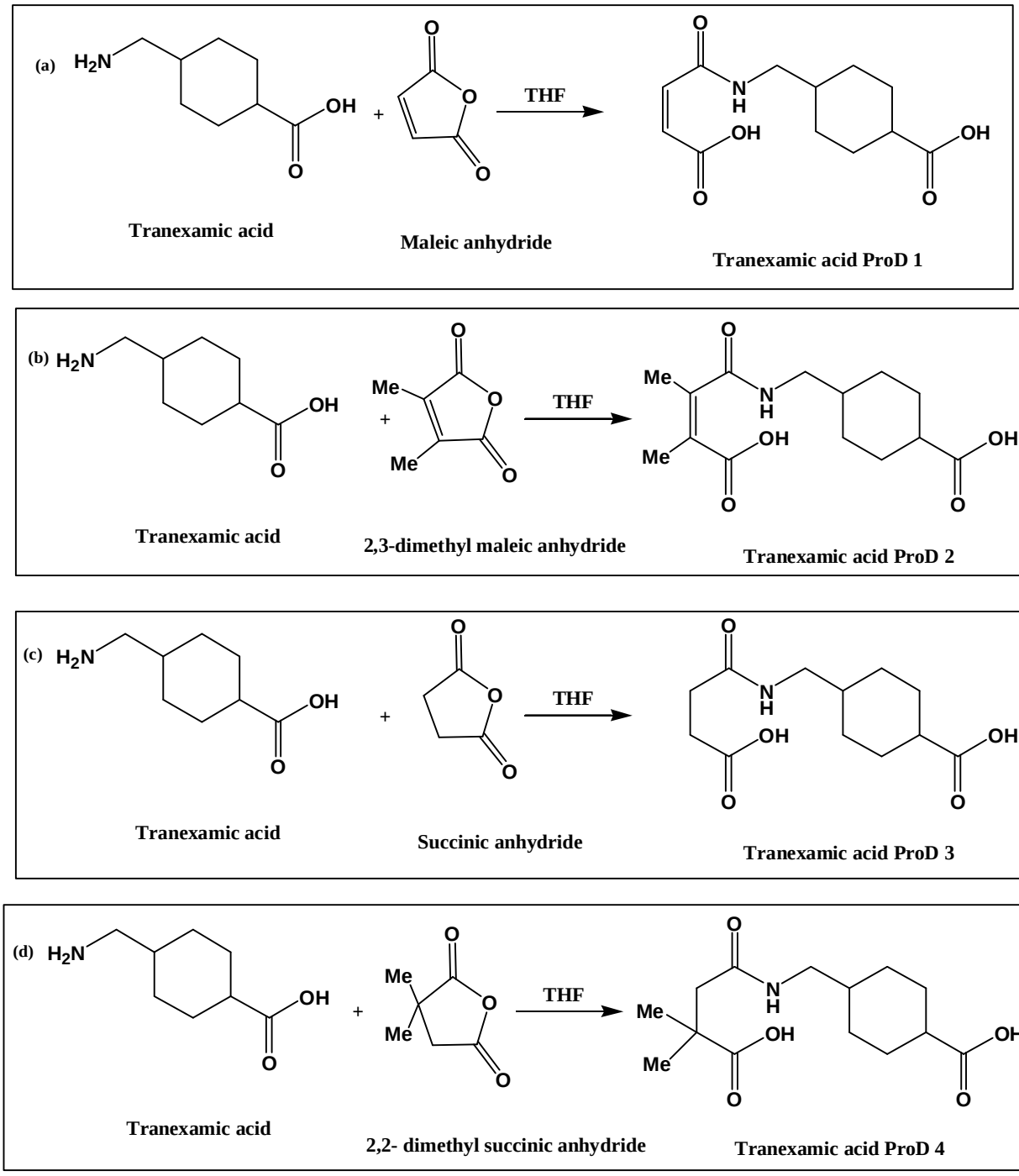

Scheme 1: Synthesis of (a) tranexamic acid **ProD 1**, (b) tranexamic acid **ProD 2**, (c) tranexamic acid **ProD 3** and (d) tranexamic acid **ProD 4.**

3.3.2 *Paracetamol prodrugs (Scheme 2)*

In a 250 ml round-bottom flask paracetamol (20 mmol) was dissolved in ether (100 ml), 1.6g of sodium hydride was added, the resulting solution was stirred for 30 minutes then 20 mmol) of maleic anhydride, succinic anhydride or glutaric anhydride was slowly added to the mixture, then the mixture was stirred overnight. 1N HCl (50 ml) was added while the round-bottom flask is setting in an ice bath. The aqueous layer was extracted with ether (90 ml) and the combined ether layer was dried over MgSO4 anhydrous, filtered and evaporated to dryness. The solid product was washed with hexane and dried to yield off-white solid. Reaction of paracetamol with maleic anhydride, succinic anhydride or glutaric anhydride provided paracetamol **ProD 1, ProD 2, ProD 3** respectively with yield 91% (4.5g) for paracetamol **ProD 2** and 88% (4.6 g) for paracetamol **ProD 3**. M.P. 70 C^o and 102 C^o for paracetamol **ProD 2** and **ProD 3**, respectively.

Paracetamol **ProD 1** was not stable; it was readily hydrolyzed to paracetamol and maleic anhydride before the ending of reaction.

Paracetamol **ProD 2**. ^{1}H-NMR δ (ppm) CD_3OD- 2.05 (s, 3H, $\underline{CH_3}$-CONH), 2.7 (t, 2H, J = 4 Hz, $\underline{CH_2}$-CH_2), 2.8 (t, 2H, J = 4 Hz, CH_2-$\underline{CH_2}$), 7.0 (d, 2H, J = 12.4 Hz, aromatic), 7.3 (d, 2H, J = 8 Hz, aromatic). IR (KBr/ν_{max} cm^{-1}) 1739 (C=O), 1668 (C=O), 1548 (C=C), 1510, 1280, 1260, 1151. *m/z* 252.0867 $(M+1)^+$.

Paracetamol **ProD 3**. ^{1}H-NMR δ (ppm) CD3OD- 2.0 (m, 2H, CH_2-$\underline{CH_2}$-CH_2), 2.1 (s, 3H, $\underline{CH_3}$-CONH), 2.44 (t, J = 4 Hz, 2H, CH_2-$\underline{CH_2}$-COOH), 2.63 (t, J = 4 Hz, 2H, ArOOC-$\underline{CH_2}$-CH_2), 7.02 (d, 2H, J = 8 Hz, aromatic), 7.5 (d, 2H, J = 8 Hz, aromatic). IR (KBr/ν_{max} cm^{-1}) 1748 (C=O), 1704 (C=O), 1556 (C=C), 1441, 1380. *m/z* 266.1075 $(M+1)^+$.

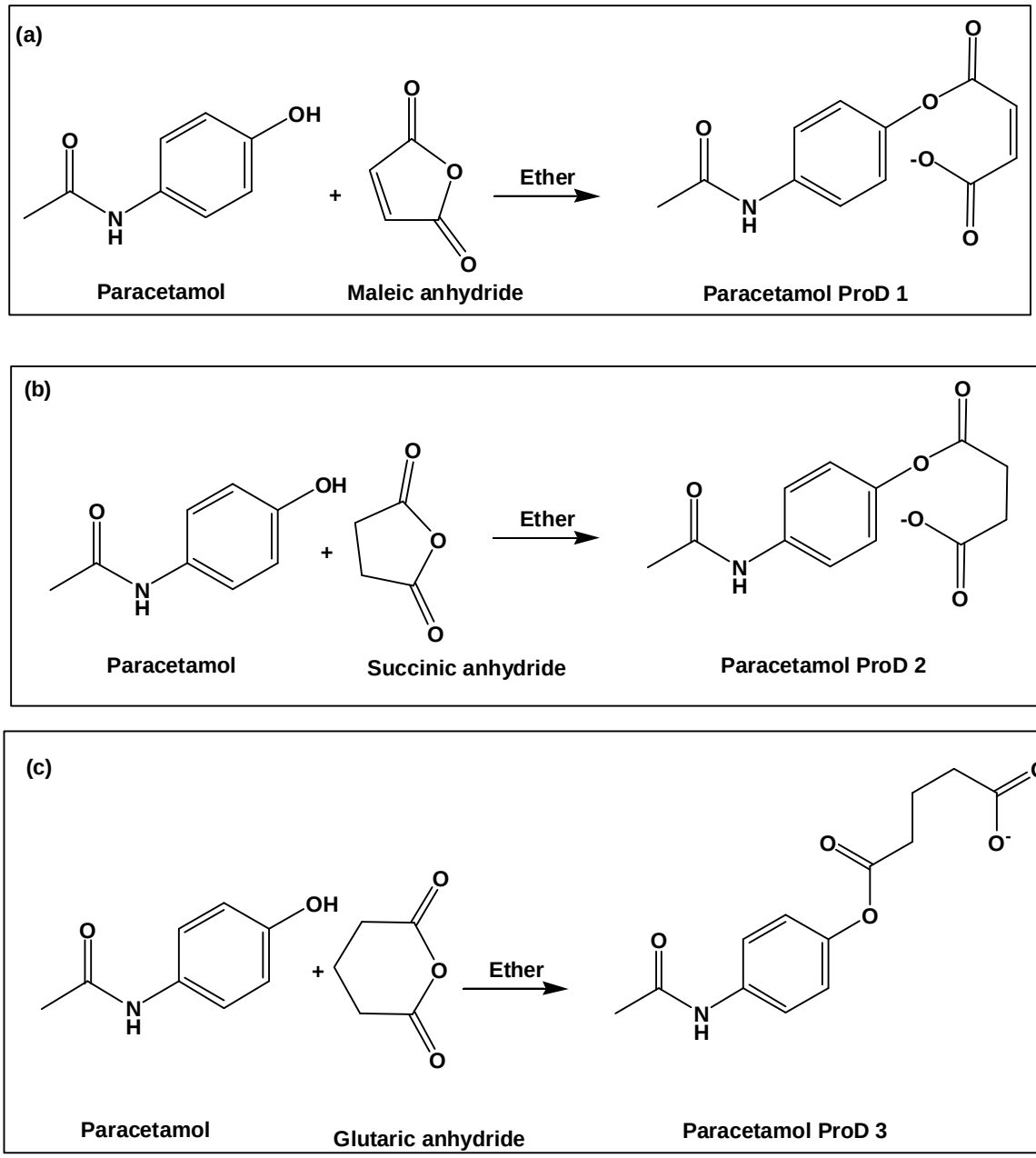

Scheme 2: Synthesis of (a) paracetamol **ProD 1**, (b) paracetamol **ProD 2**, (c) paracetamol **ProD 3**.

3.4 Kinetic Methods

3.4.1 Buffer Preparation

6.8 g potassium dihydrogen phosphate were dissolve in 900 ml water for HPLC, the pH of buffers pH 2 and pH 3 was adjusted by diluted o- phosphoric acid and water was added to a final volume of 1000 ml (0.05M). The same procedure was done for the preparation of buffers pH 5 and 7.4, however, the required pH was adjusted using 1 N NaOH.

Intra-conversion of 500 ppm tranexamic acid **ProD 1-4** solutions, in 1N HCl, buffer pH 2, buffer pH 5 or buffer pH 7.4, to its parent drug, tranexamic acid, was followed by HPLC at a wavelength of 220 nm. Conversion reactions were run mostly at 37.0 ˚C. Intra-conversion of 500 ppm paracetamol **ProD 2**, **ProD 3** solutions, in 1N HCl, buffer pH 3 and buffer pH 7.4, to its parent drug, paracetamol, was followed by HPLC at a wavelength of 245 nm. Conversion reactions were run mostly at 37.0 ˚C.

3.4.2 Calibration curve

A 100 ml stock solution of tranexamic acid **ProD 1-4** with a final concentration of 500 ppm were prepared by dissolving 50 mg from each prodrug in 100 ml methanol. The following diluted solutions were prepared from the stock solution: 100, 200, 300 and 400 ppm. Each solution was then injected to the HPLC apparatus using 6 mm x 250 mm, 5 µm C18 XBridge ® column, mobile phase contains 11 g anhydrous sodium dihydrogen phosphate, 1.4 g Sodium Lauryl Sulfate, 5 ml triethylamine dissolved in 600 ml water and 400 ml methanol (pH 2.5 using diluted phosphoric acid), a flow rate of 0.9 ml min^{-1} and UV detection at a wavelength of 220 nm.

Peak area vs. concentration of the pharmaceutical (ppm) was then plotted, and R^2 of the plot was recorded.

A 100 ml stock solution of paracetamol **ProD 2** and **ProD 3** with a final concentration of 500 ppm were prepared by dissolving 50 mg from each prodrug in 100 ml methanol. The following diluted solutions were prepared from the stock solution: 100, 200, 300 and 400 ppm. Each solution was then injected to the HPLC apparatus using 6 mm x 250 mm, 5

µm C18 XBridge ® column, mobile phase water: acetonitrile (80:20), a flow rate of 1 ml min^{-1} and UV detection at a wavelength of 245 nm.

Peak area vs. concentration of the pharmaceutical (ppm) was then plotted, and R^2 of the plot was recorded.

3.5.3 Preparation of standard and sample solution

3.5.3.1 Tranexamic acid prodrugs

A 500 ppm of standard tranexamic acid was prepared by dissolving 50 mg of tranexamic acid in 100 ml of 1N HCl, buffer pH 2, buffer pH 5 or buffer pH 7.4, then each sample was injected into HPLC to detect the retention time of tranexamic acid.

A 500 ppm of standard linker (maleic anhydride, 2,3-dimethyl maleic anhydride, succinic anhydride and 2,2-dimethyl succinic anhydride) was prepared by dissolving 50 mg of each linker in 100 ml of 1N HCl, buffer pH 2, buffer pH 5 or buffer pH 7.4, then each sample was injected into HPLC to determine the retention time of linker.

A 500 ppm of each tranexamic acid **ProD 1-4** was prepared by dissolving 50 mg of the tranexamic acid **ProD 1-4** in 100 ml of 1N HCl, buffer pH 2, buffer pH 5 or buffer pH 7.4 then each sample was injected into the HPLC to determine the retention time.

The progression of reaction was followed by monitoring the disappearance of the prodrug and appearance of tranexamic acid and linker maleic anhydride, 2,3-dimethyl maleic anhydride, succinic anhydride, 2,2-dimethyl succinic anhydride with. time.

3.5.3.2 Paracetamol prodrugs

A 500 ppm of standard paracetamol was prepared by dissolving 50mg of paracetamol in 100 ml of 1N HCl, buffer pH 3 and buffer pH 7.4, then each sample was injected into the HPLC to determine the retention time of paracetamol.

A 500 ppm of paracetamol **ProD 2** and **ProD 3** was prepared by dissolving 50mg of paracetamol **ProD 2** and **ProD 3** in 100 ml of 1N HCl, buffer pH 3 and buffer pH 7.4 then each sample was injected into the HPLC to determine the retention time of paracetamol **ProD 2** and **ProD 3**.

The progression of reaction was followed by monitoring the disappearance of prodrug and the appearance of parent drug (paracetamol) with time.

Results and Discussion

Chapter Four

4. Results and Discussion

Trnexamic acid and paracetamol prodrugs were synthesized, purified and characterized using different spectroscopic and chromatographic techniques.

4.1. Characterization

Tranexamic acid, tranexamic acid **ProD 1- 4**, paracetamol **ProD 2** and paracetamol **ProD 3** were characterized by FT-IR, LC-MS and ^{1}H-NMR spectroscopy.

Tranexamic acid ($C_8H_{15}NO_2$). The IR spectrum (Figure 4.1 a) shows an absorbance at 1642 cm^{-1} corresponds to C=O, 1425 cm^{-1}, 1280 cm^{-1}, 1256 cm^{-1}, 1132 cm^{-1}, 1058 cm^{-1}. A high resolution LC-MS (Figure 4.1 b) at the ESI (positive mode) shows a protonated peak at *m*/*z* 158.1176 $(M+1)^{+}$, an adduct of $[M+Na]^{+}$ was appeared at *m*/*z* of 180.0993. The ^{1}H-NMR (Figure 4.1 c) peaks occur at 1.06 ppm (q, 2H, CH-$\underline{CH_2}$-CH_2), 1.40 ppm (q, 2H, CH-$\underline{CH_2}$-CH_2), 1.54 ppm (m, 1H, CH_2-$\underline{CH}$-CH_2-CH_2), 1.84 ppm (m, 2H, CH_2-$\underline{CH_2}$-CH), 2.02 ppm (m, 2H, CH_2-$\underline{CH_2}$-CH), 2.22 ppm (m, 1H, CH_2-$\underline{CH}$-CH_2-CH2), 3.17 ppm (d, 2H, $\underline{CH_2}$-N).

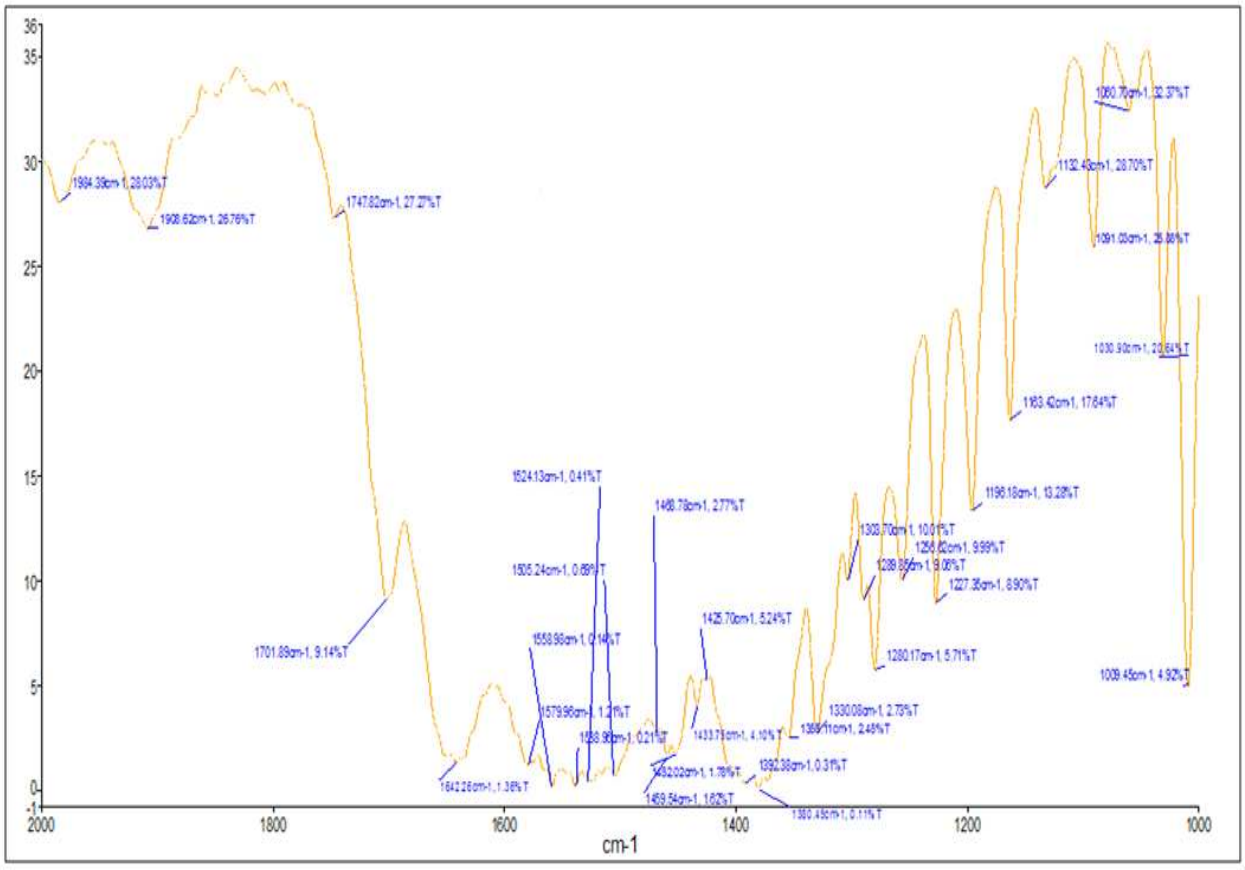

Figure 4.1 a. FT-IR spectrum of tranexamic acid.

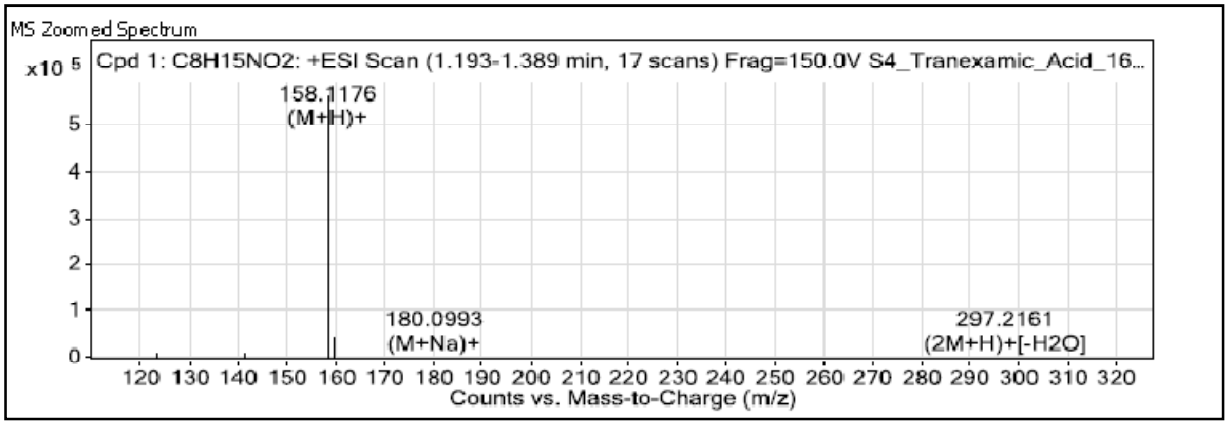

Figure 4.1 b. LC-MS spectrum of tranexamic acid.

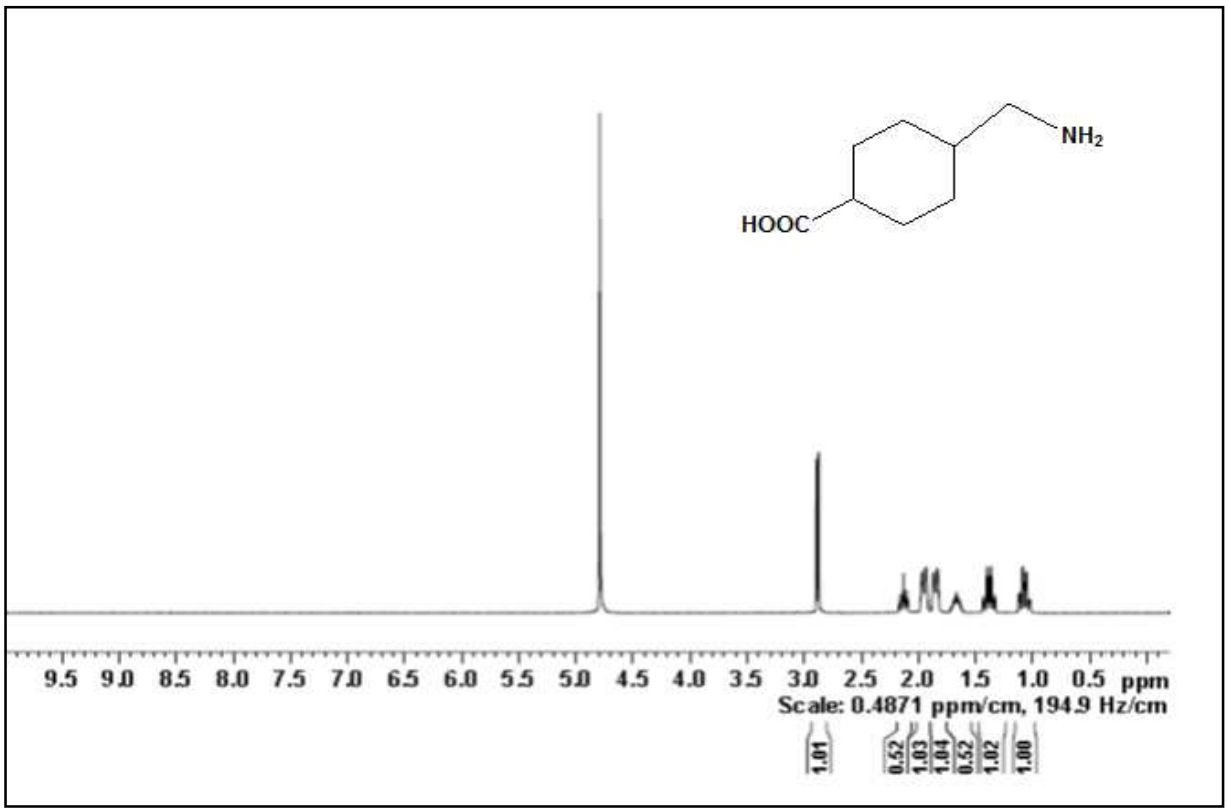

Figure 4.1 c. ^{1}H-NMR spectrum of tranexamic acid in CD_3OD.

Tranexamic acid ProD 1 ($C_{12}H_{17}NO_5$). The zoomed IR spectrum (Figure 4.2 a) shows an additional signals with absorbance 1712 cm^{-1}, 1643 cm^{-1} corresponds to C=O of the maleate moiety,. A high resolution LC-MS (Figure 4.2 b) shows a protonated peak at *m*/*z* 256.1179 $(M+1)^{+}$, an adduct of $[M+Na]^{+}$ was appeared at *m*/*z* of 278.0992. The ^{1}H-NMR (Figure 4.2 c) the alkene cis proton show doublet peaks at 6.25. 6.45 with coupling constant of 14 Hz, indicate the cis arrangement of these protons.

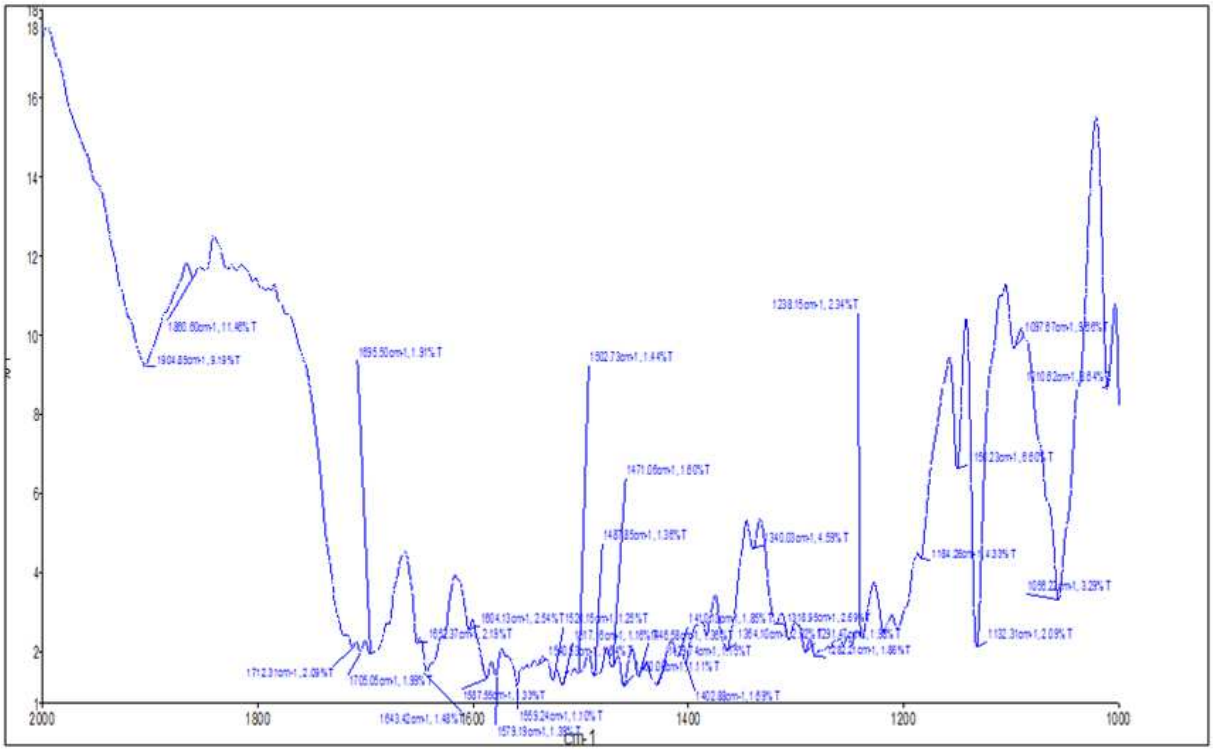

Figure 4.2 a. FT-IR spectrum of tranexamic acid **ProD 1**.

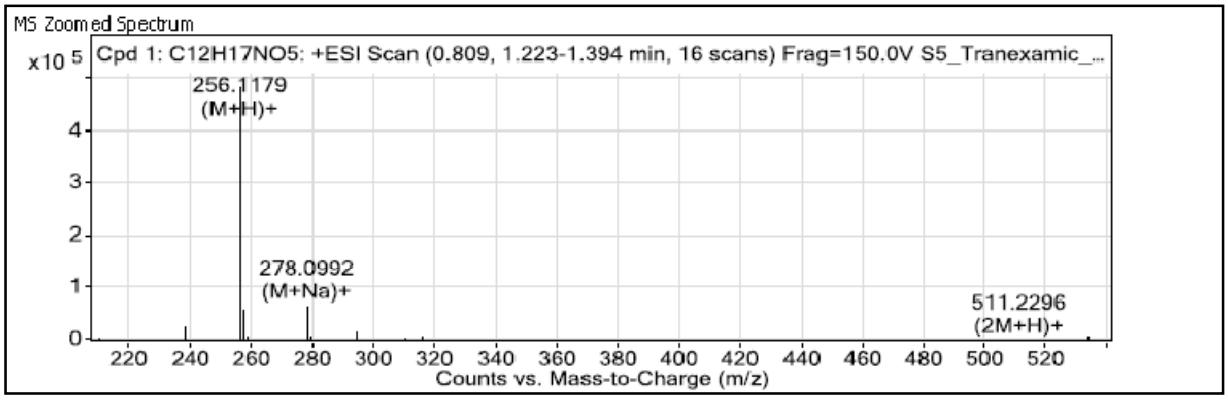

Figure 4.2 b. LC-MS spectrum of tranexamic acid **ProD 1**.

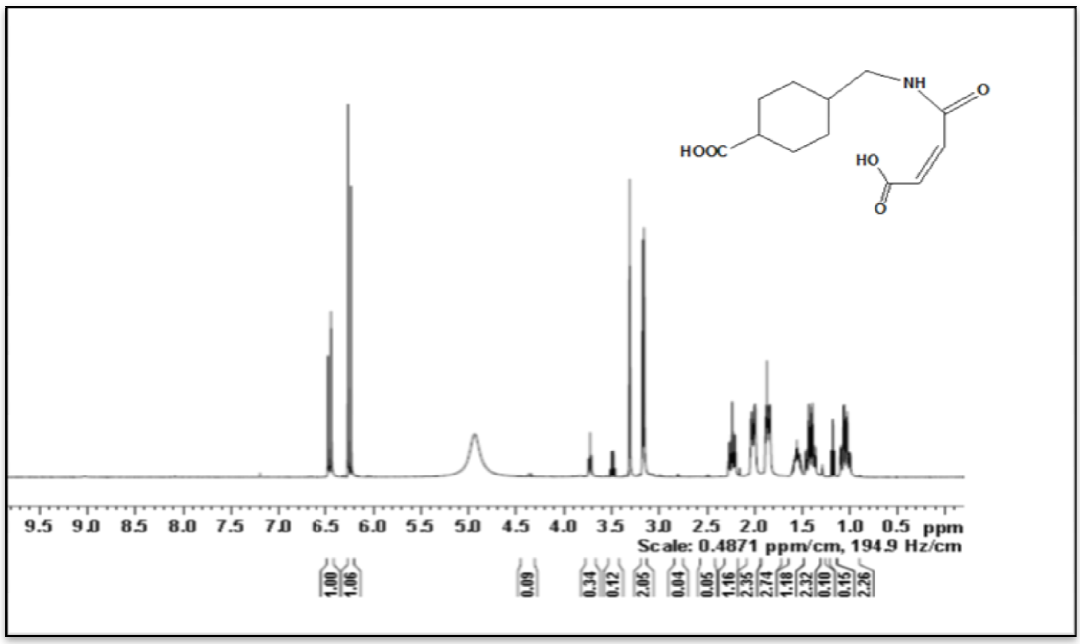

Figure 4.2 c. ^{1}H-NMR spectrum of tranexamic acid ProD 1 **in CD_3OD**.

Tranexamic acid ProD 2 ($C_{14}H_{21}NO_5$). The zoomed IR spectrum (Figure 4.3 a) shows an absorbance of the additional carbonyl group (C=O) for the dimethyl maleate moiety at 1751 cm^{-1}, 1646 cm^{-1} , . A high resolution LC-MS (Figure 4.3 b) shows a protonated peak at *m*/*z* 566.2905 $(2M+1)^{+}$. The ^{1}H-NMR (Figure 4.3 c) an additional singlet peak occur at 1.93ppm represent the two methyl groups on C=C of the dimethyl maleate moiety.

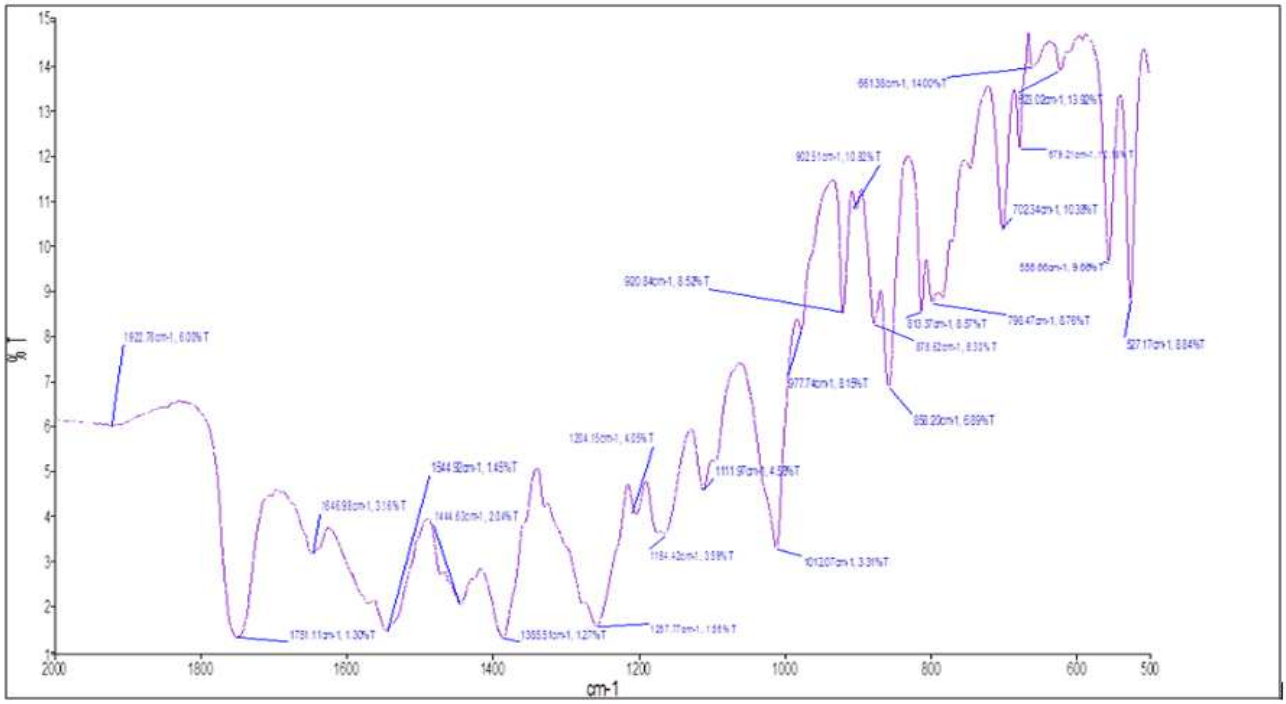

Figure 4.3 a. FT-IR spectrum of tranexamic acid **ProD 2**.

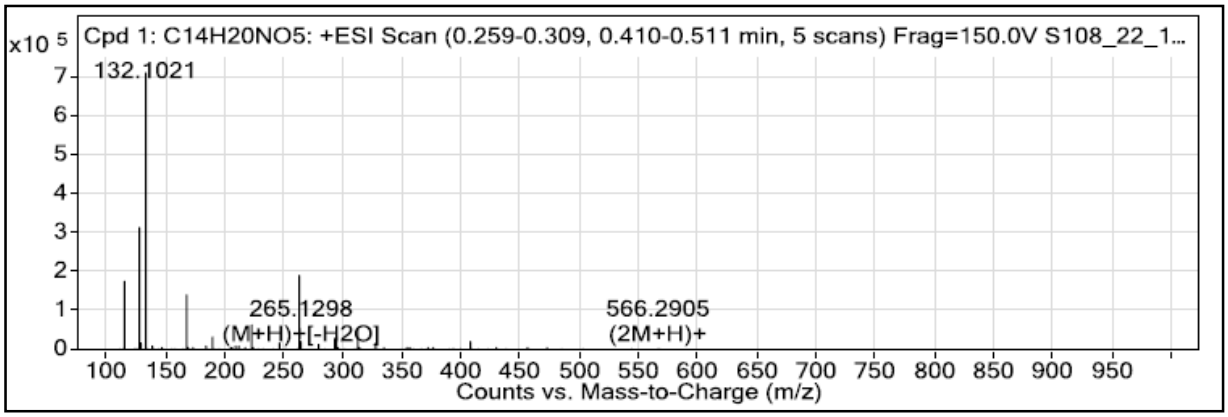

Figure 4.2 b. LC-MS spectrum of tranexamic acid **ProD 2**.

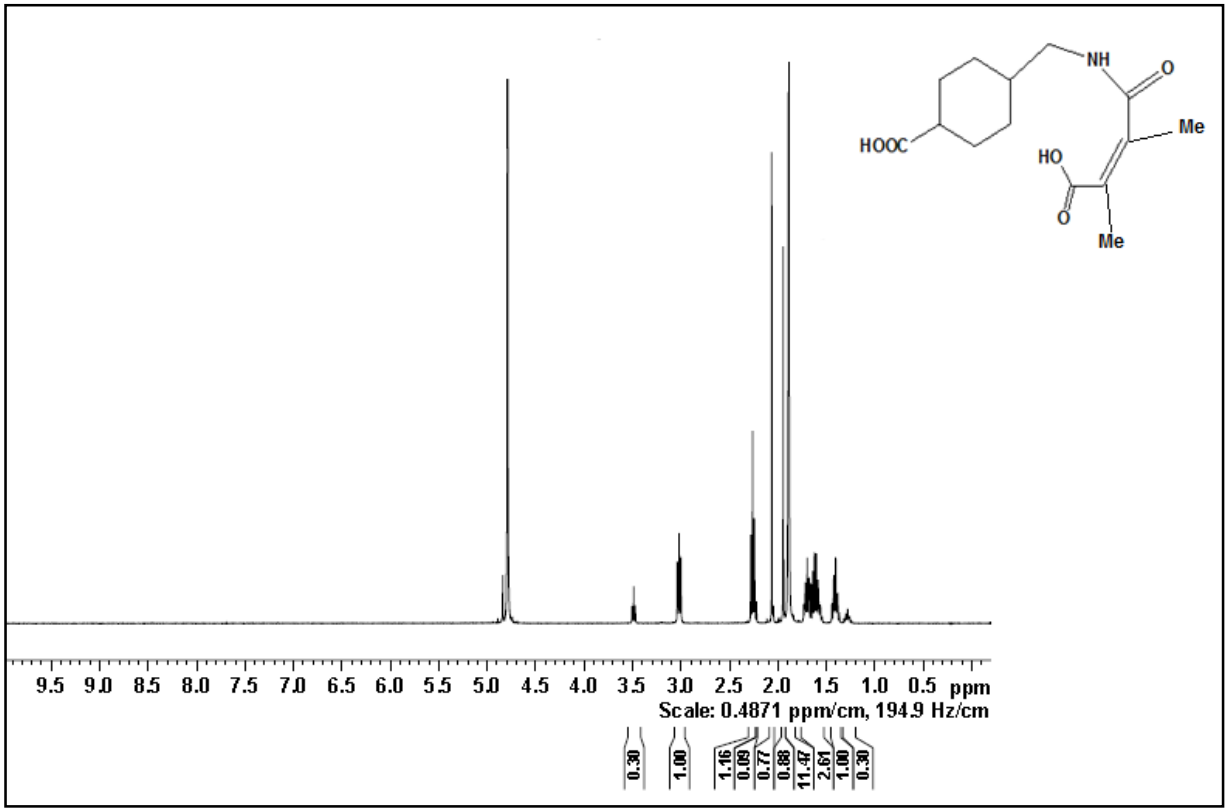

Figure 4.3 c. ^{1}H-NMR spectrum of tranexamic acid **ProD 2** in D_2O.

Tranexamic acid ProD 3 ($C_{12}H_{19}NO_5$). The IR spectrum (Figure 4.4 a) shows an absorbance at 1742 cm^{-11} corresponds to the additional carbonyl group (C=O) for the succinate moiety,. A high resolution LC-MS (Figure 4.4 b) shows a protonated peak at *m/z* 507.3454 $(2M+1)^{+}$. The ^{1}H-NMR (Figure 4.4 c) shows an additional a triplet signal for the succinate moiety protons occur at 2.44ppm with coupling constant of 4.8 Hz and at 2.5 ppm with coupling constant of 4.0 Hz.

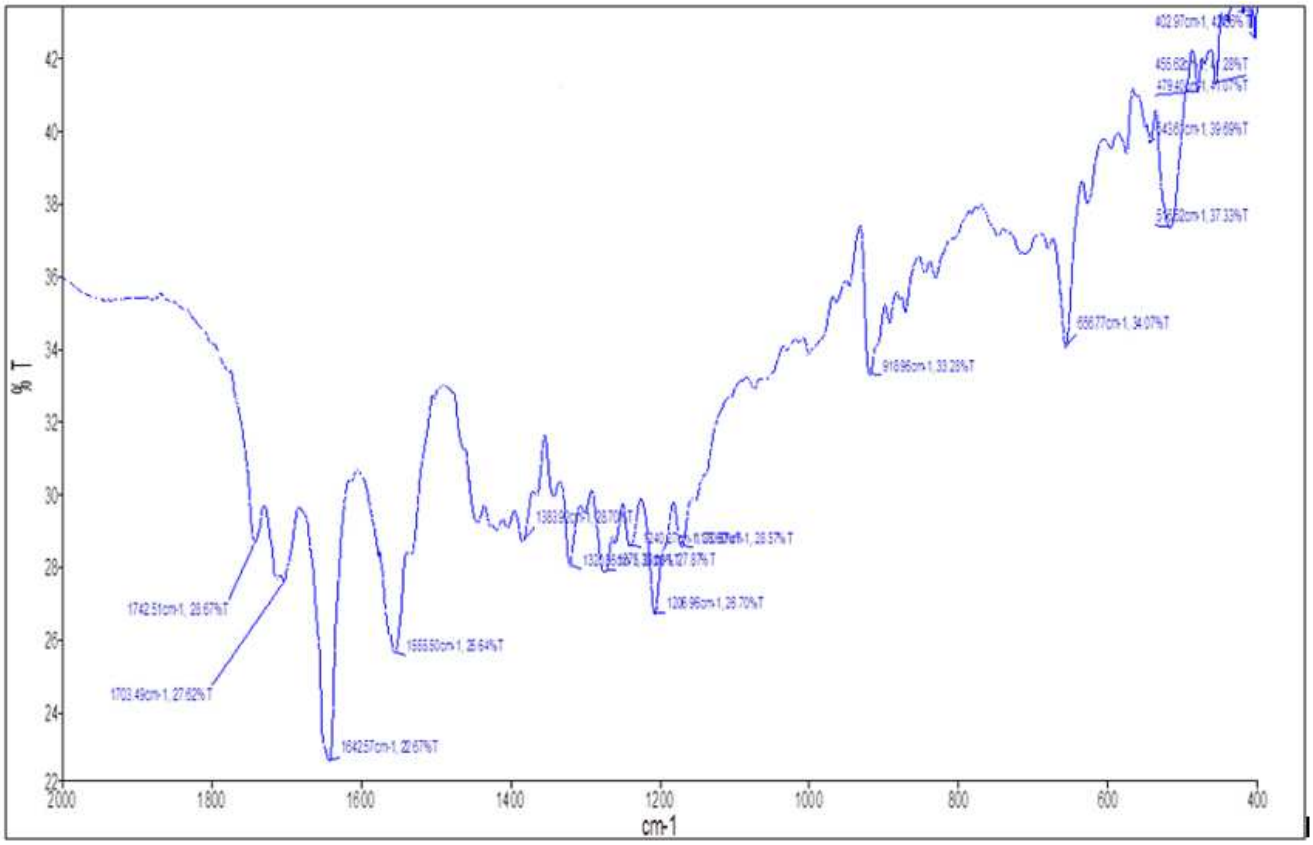

Figure 4.4 a. FT-IR spectrum of tranexamic acid **ProD 3**.

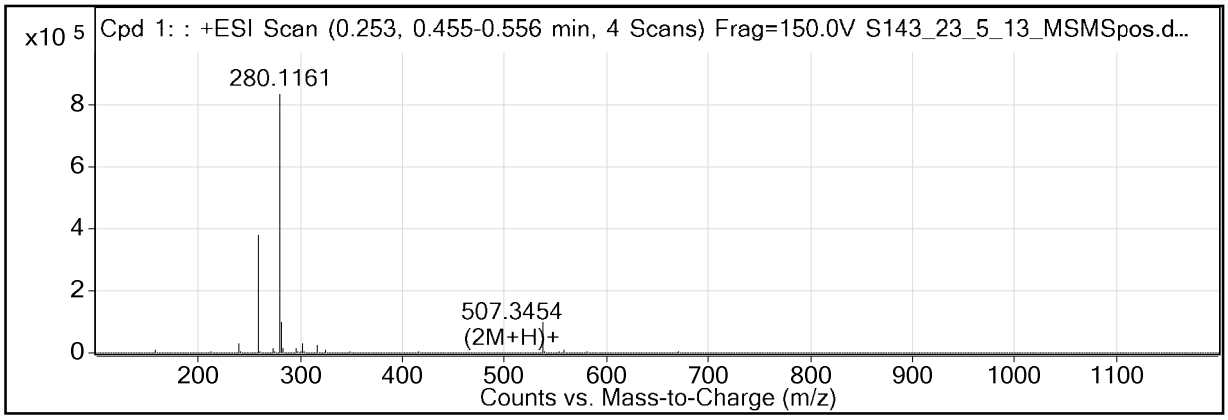

Figure 4.4 b. LC-MS spectrum of tranexamic acid **ProD 3**.

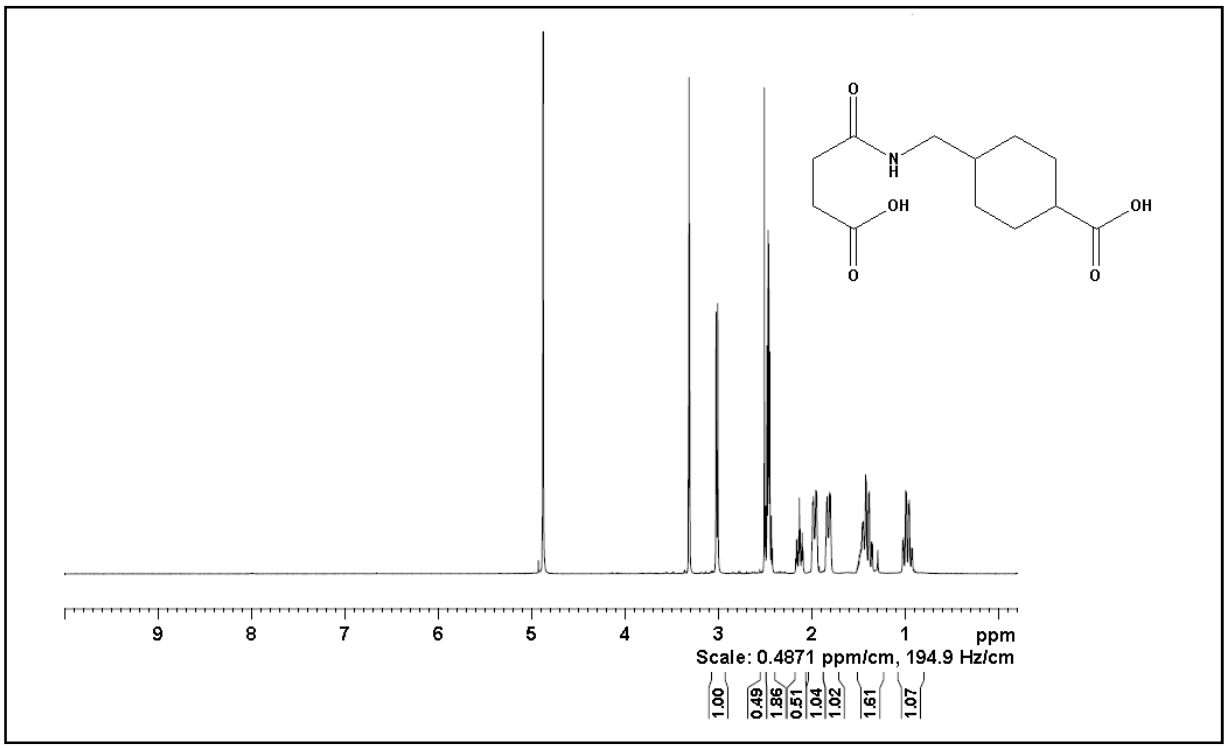

Figure 4.4 c. ^{1}H-NMR spectrum of tranexamic acid **ProD 3** in CD_3OD.

Tranexamic acid ProD 4 ($C_{14}H_{23}NO_5$). The zoomed IR spectrum (Figure 4.5 a) shows an absorbance at 1750 cm^{-1}corresponds to the carbonyl groub (C=O) of dimetyl succinate moiety. A high resolution LC-MS (Figure 4.5 b) shows a protonated peak at *m*/*z* 286.1627 $(M+1)^{+}$. ^{1}H-NMR (Figure 4.5 c) the protons for the two methyl groups of the dimethyl succinate moiety show a singlet peak at 1.21 ppm with coupling constant of 20 Hz.

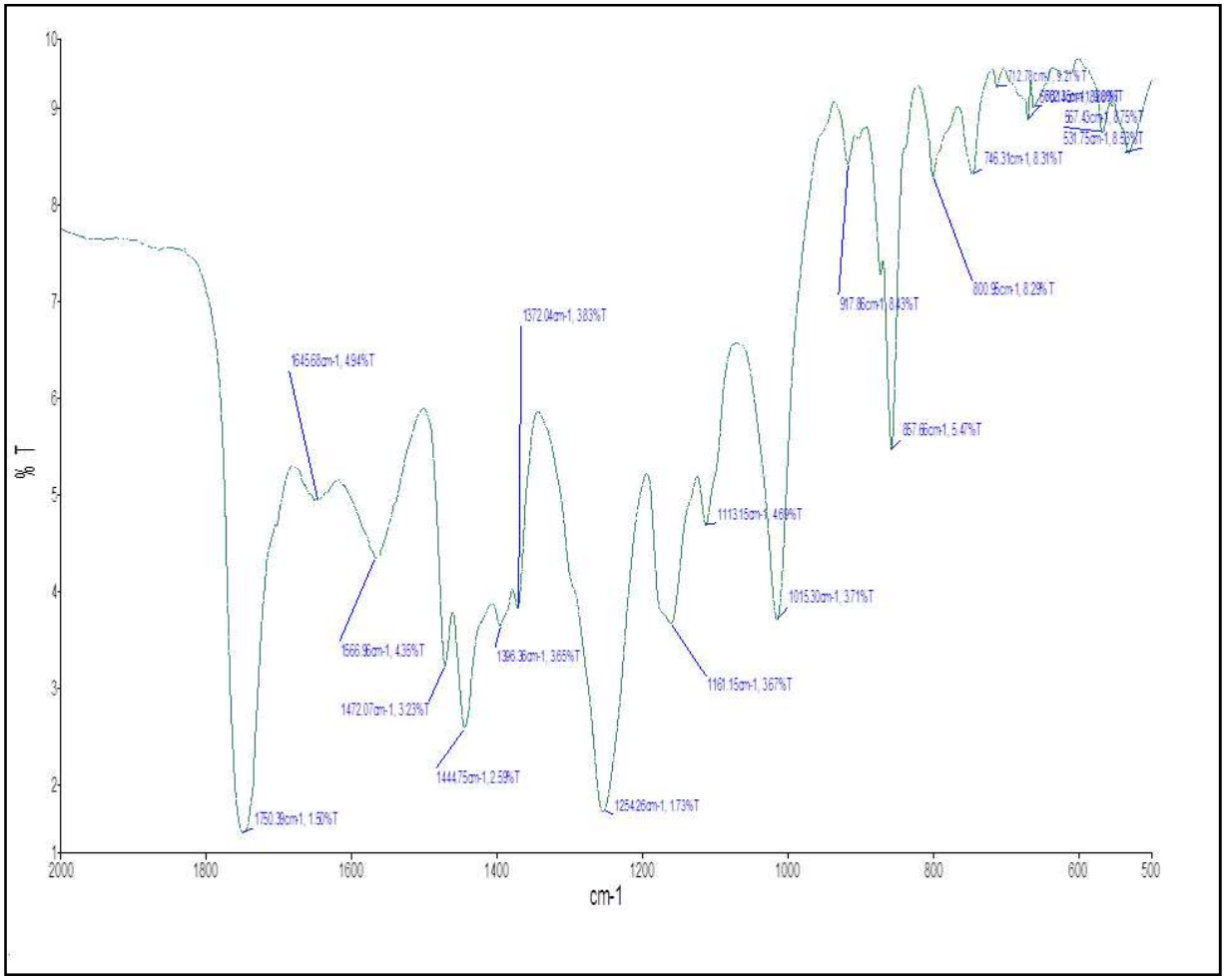

Figure 4.5 a. FT-IR spectrum of tranexamic acid **ProD 4**.

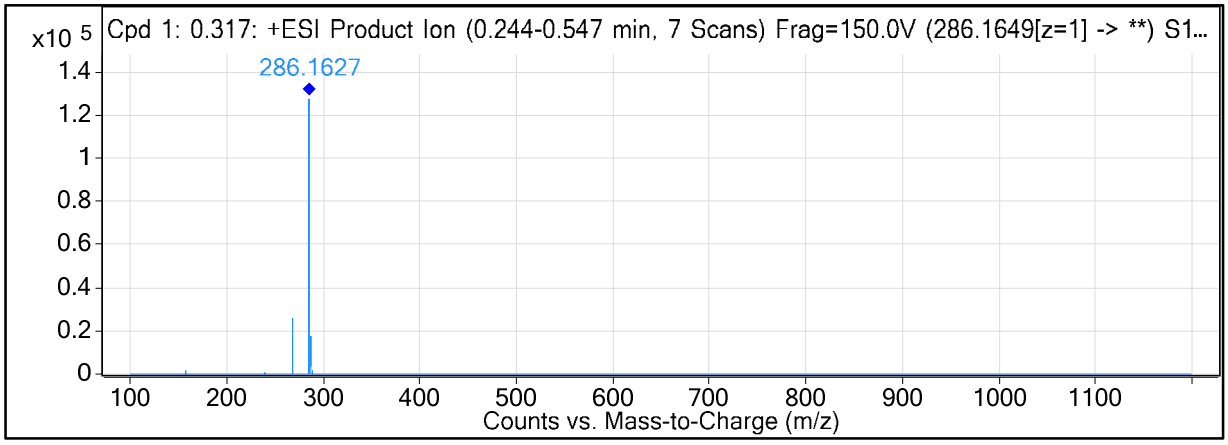

Figure 4.5 b. LC- MS spectrum of tranexamic acid **ProD 4**.

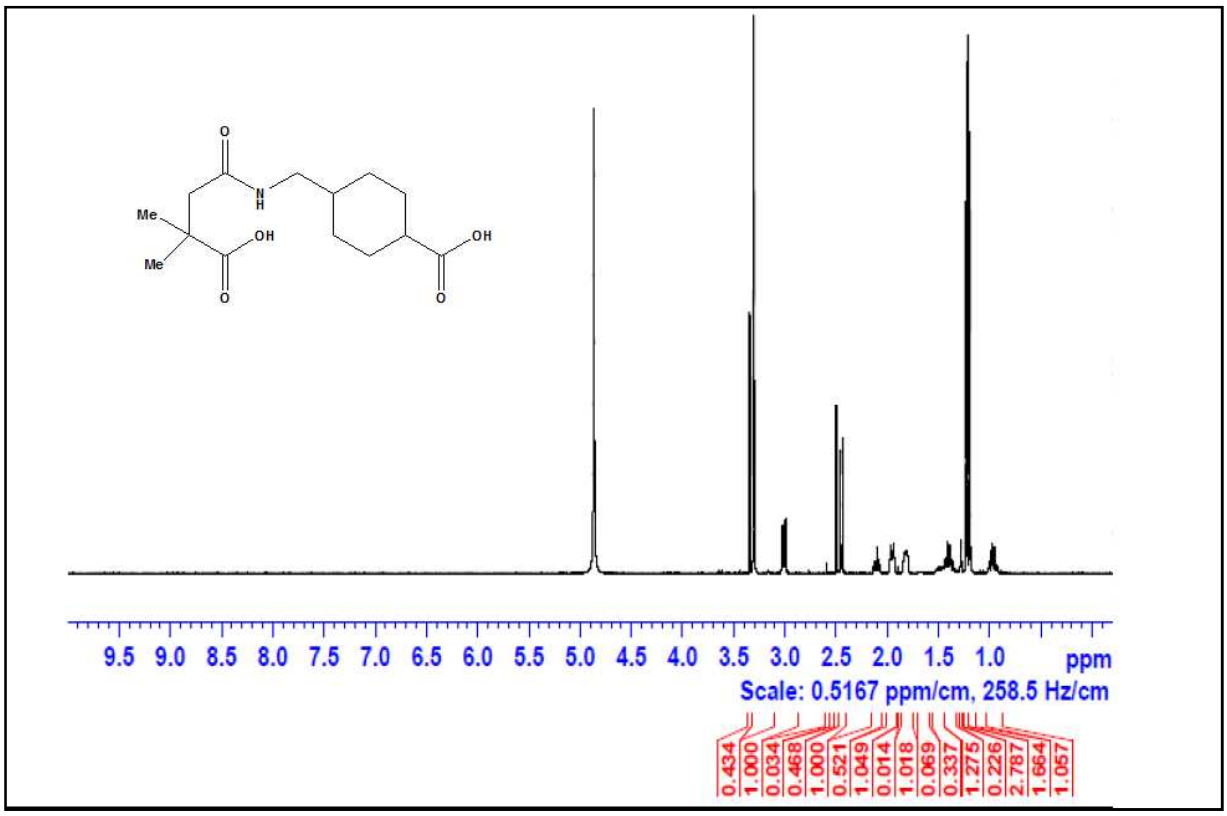

Figure 4.5 c. ^{1}H-NMR spectrum of tranexamic acid **ProD 4** in CD_3OD.

Paracetamol ($C_8H_9NO_2$)**.** The IR spectrum (Figure 4.6 a) shows an absorbance at 1612cm^{-1} corresponds to C=C and 1567 cm^{-1} corresponds to C=C. The ^{1}H-NMR (Figure 4.6 b) peaks occur at 2.1 ppm (s, 3H, $\underline{CH_3}$-CONH), 6.7 ppm (d, 2H, J = 12.4 Hz, aromatic), 7.3 ppm (d, 2H, J = 8Hz, aromatic).

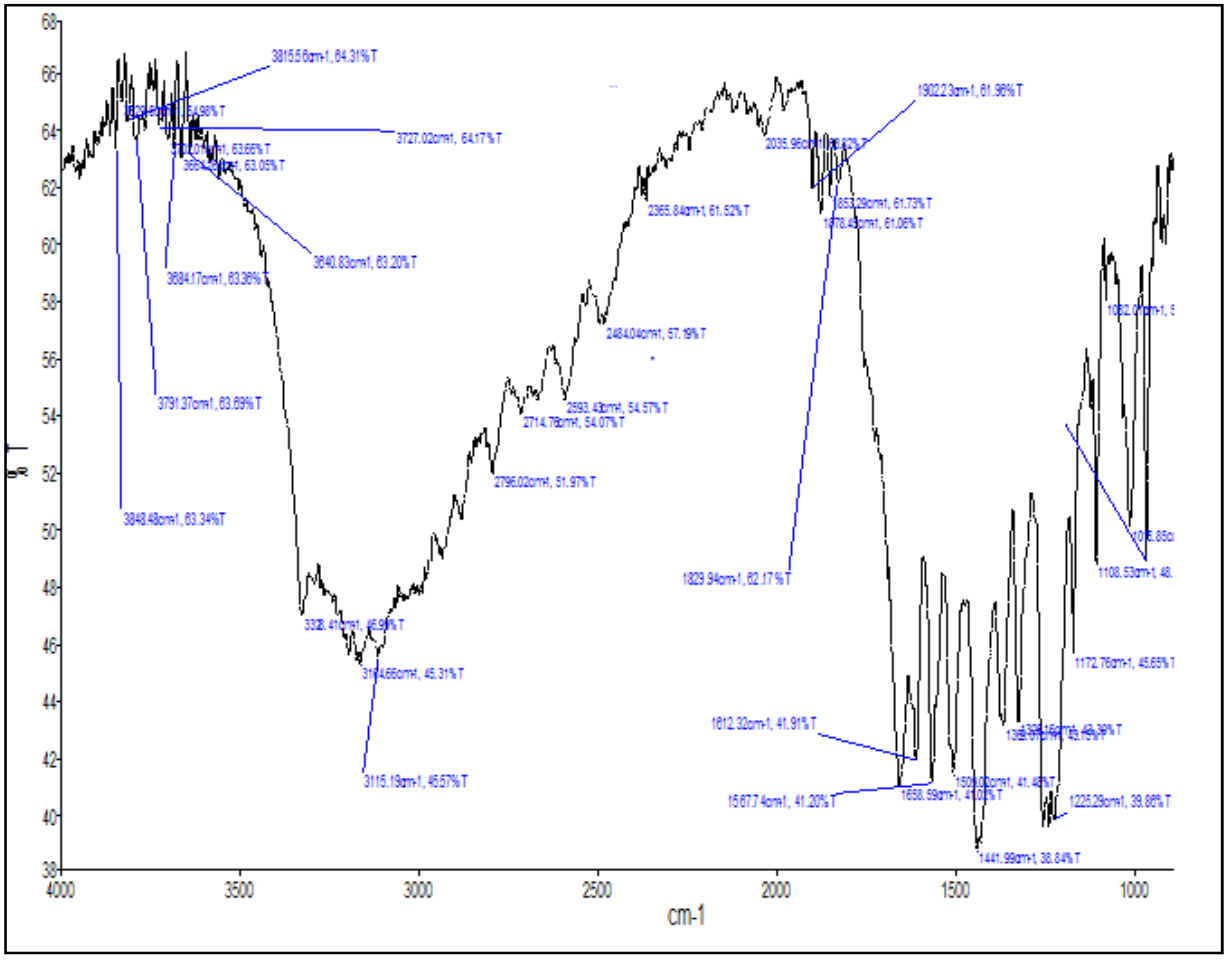

Figure 4.6 a. FT-IR spectrum of paracetamol.

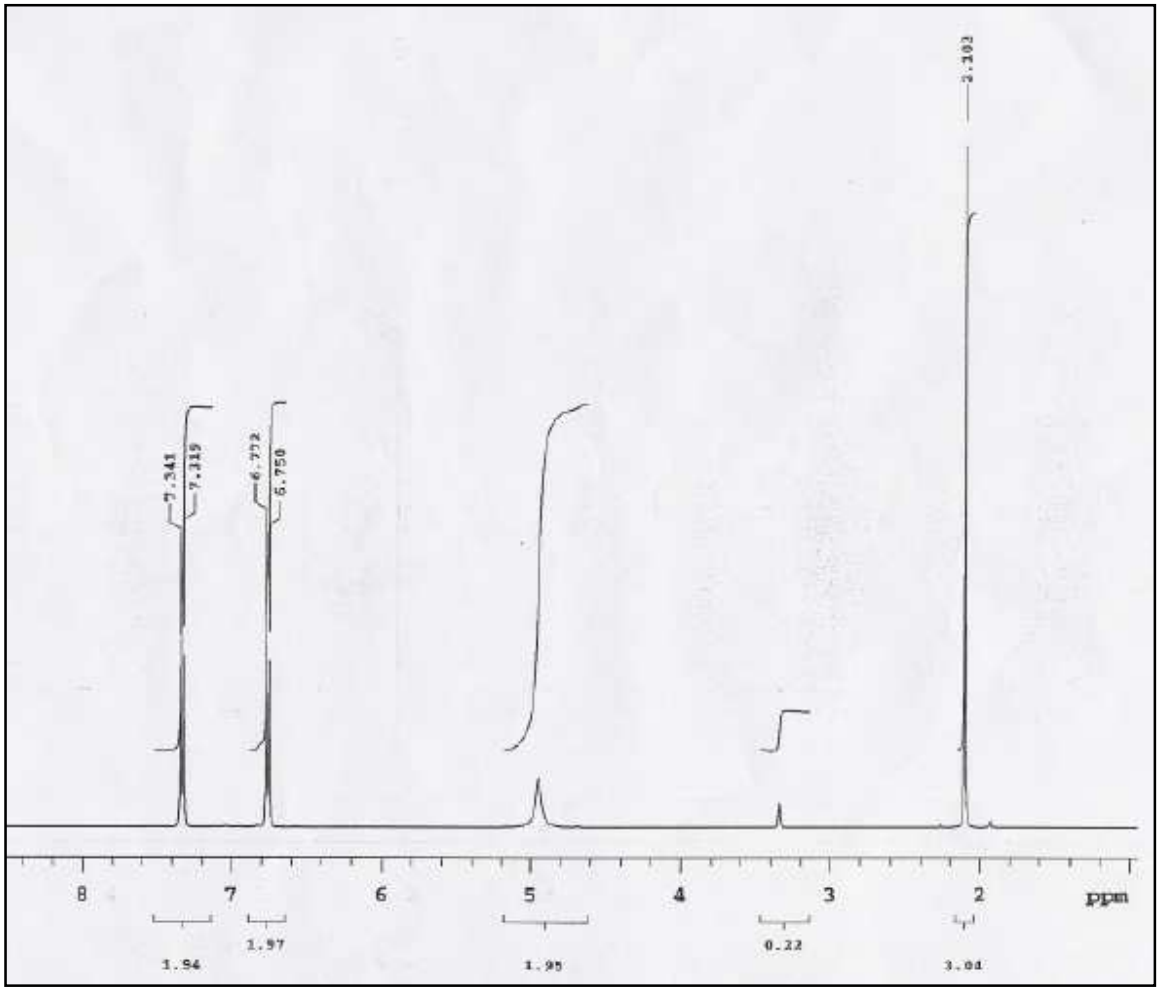

Figure 4.6 b. ^{1}H-NMR spectrum of paracetamol in CD_3OD.

Paracetamol ProD 2 ($C_{12}H_{13}NO_5$)**.** The zoomed IR spectrum (Figure 4.7 a) shows an additional signal with absorbance of 1750 cm^{-1}corresponds to carbonyl group (C=O) for the succinate moiety. A high resolution LC-MS (Figure 4.7 b) shows a protonated peak at *m/z* 252.0867 $(M+1)^+$. The ^{1}H-NMR (Figure 4.7 c) shows two additional triblet peaks occur at 2.7 ppm and 2.8 ppm with coupling constant of 4 Hz corresponding to the four protons of the succinate moiety.

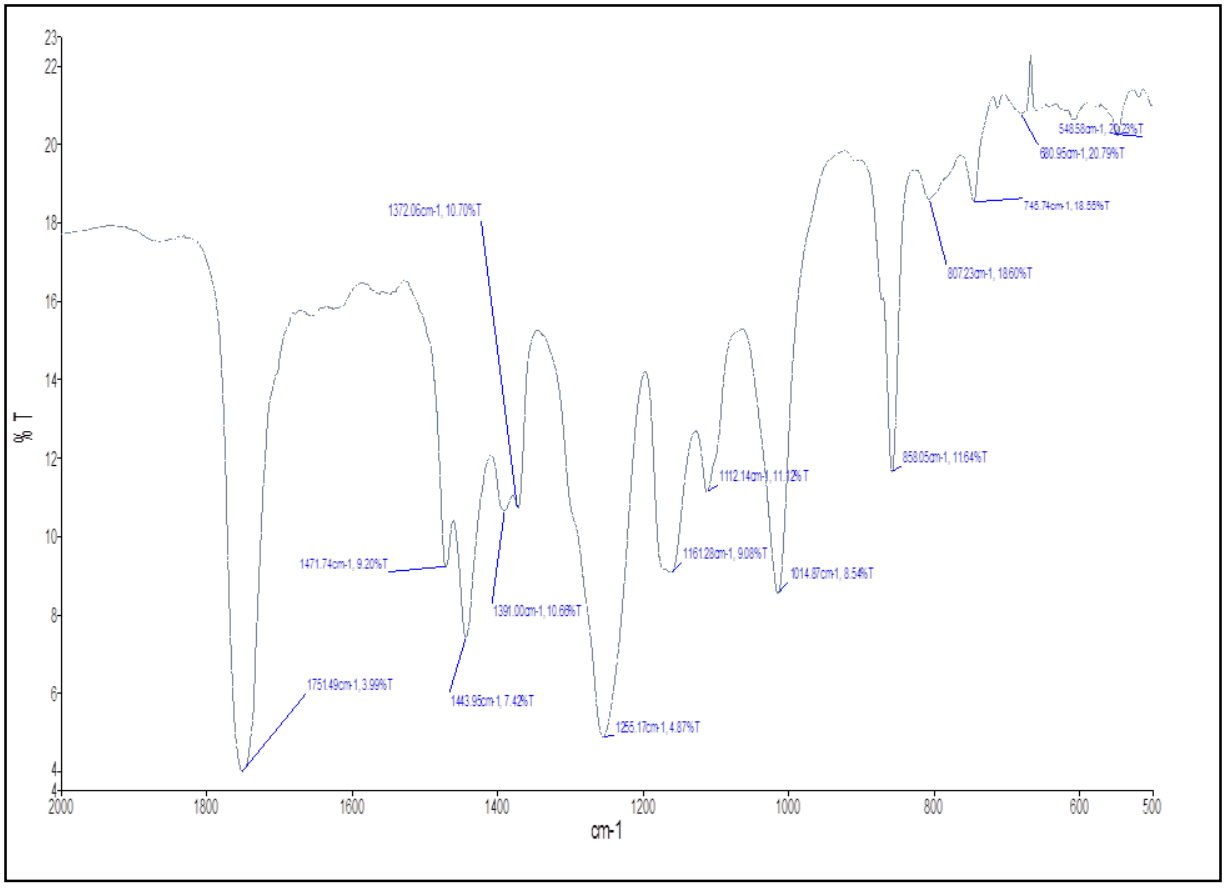

Figure 4.7 a. FT-IR spectrum of paracetamol **ProD 2**.

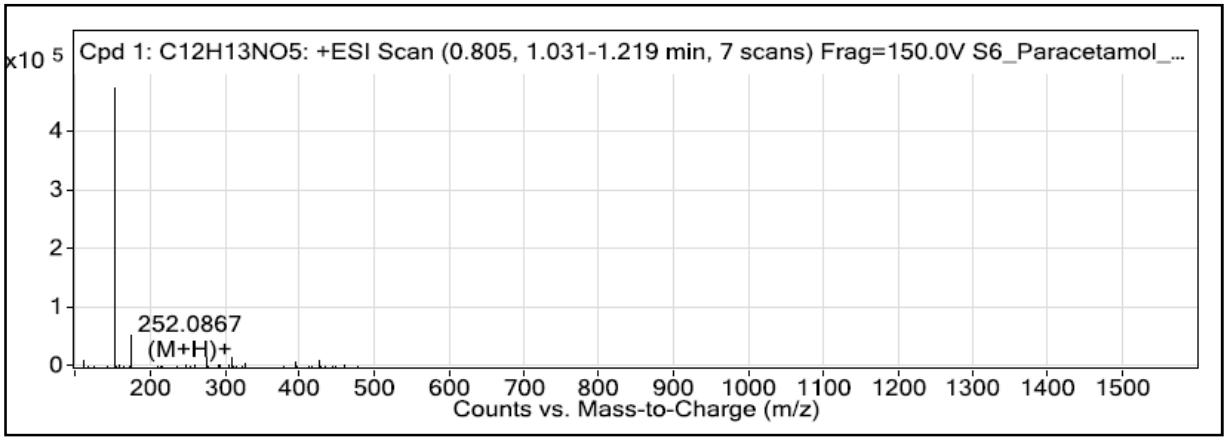

Figure 4.7 b. LC- MS spectrum of paracetamol **ProD 2**.

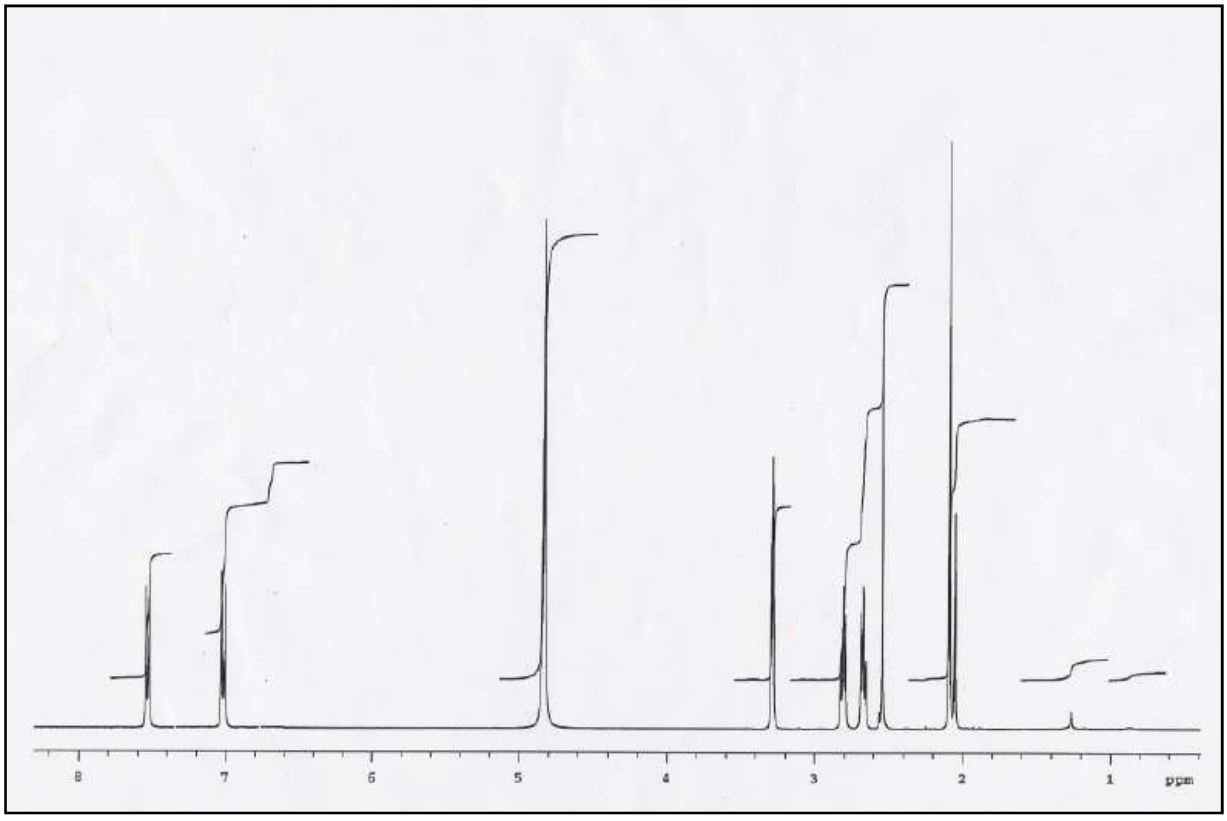

Figure 4.7 c. ^{1}H-NMR spectrum of paracetamol **ProD 2** in CD_3OD.

Paracetamol ProD 3 ($C_{13}H_{15}NO_5$). The zoomed IR spectrum (Figure 4.8 a) shows an absorbance at 1748 cm^{-1},corresponds to the additional carbonyl group (C=O) for the glutarate moiety. A high resolution LC-MS (Figure 4.8 b) shows a protonated peak at *m/z* 266.1075 $(M+1)^+$. ^{1}H-NMR (Figure 4.8 c) the six protons for the glutarate moity occur at 2.0 ppm with multiplet signal and a triplet signal at 2.44 ppm, 2.63 ppm with coupling constant of 4Hz.

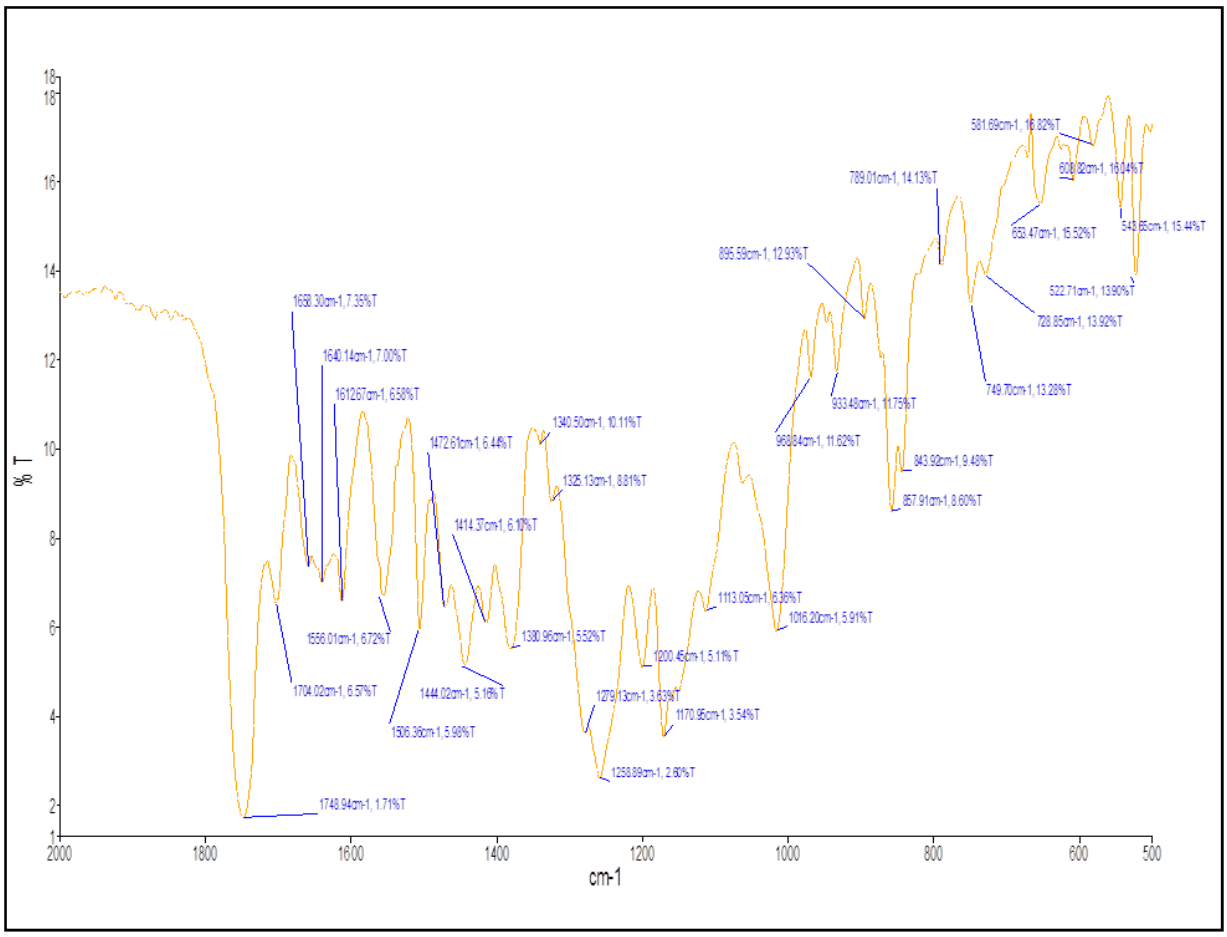

Figure 4.8 a. FT-IR spectrum of paracetamol **ProD 3**.

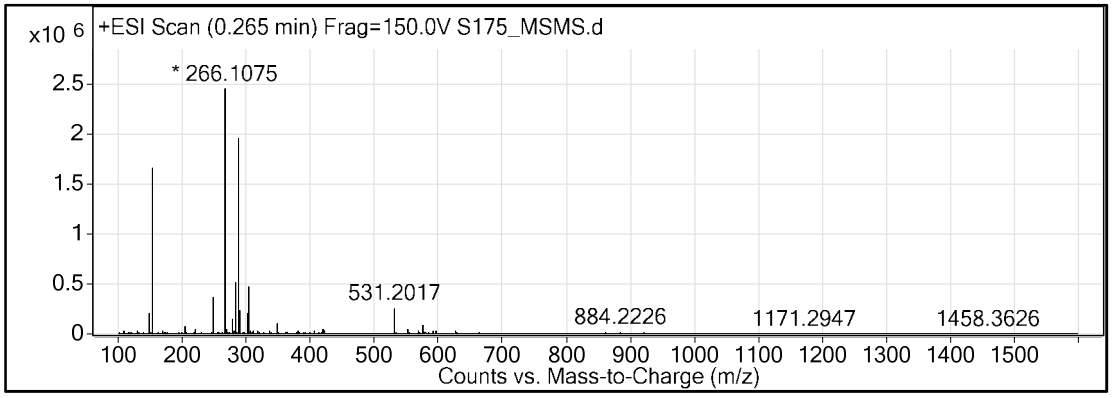

Figure 4.8 b. LC- MS spectrum of paracetamol **ProD 3**.

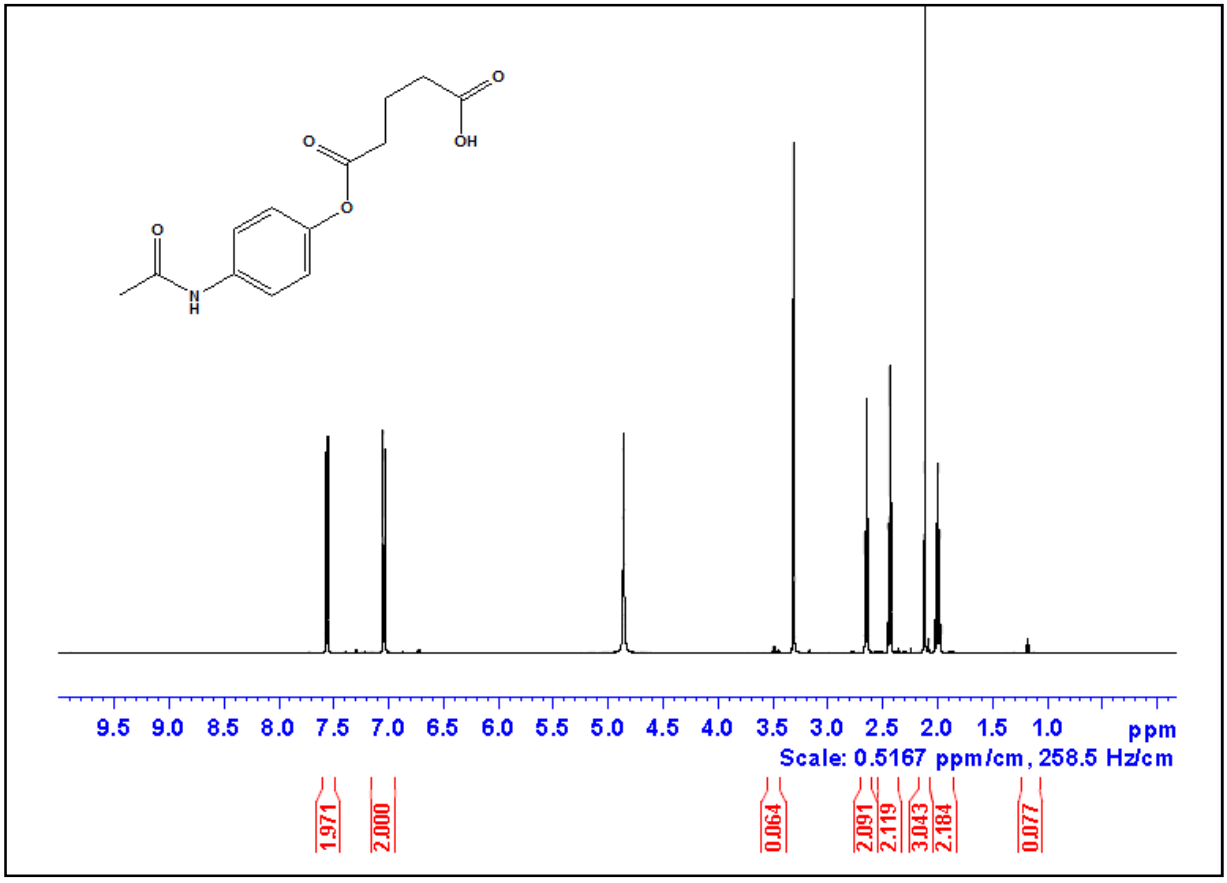

Figure 4.8 c. ^{1}H-NMR spectrum of paracetamol **ProD 3** in CD3OD.

The IR, ^{1}H-NMR and LC-MS spectral results mentioned before, confirmed that the desired prodrugs are obtained from each reaction.

4.2 Calibration curve for tranexamic acid ProD 1- 4, paracetaml ProD 2, ProD 3

In order to follow the fact of the prodrugs kinetic calibration curves were obtained by plotting the HPLC peak area versus concentration as displayed in Figure 4.9 for tranexamic acid **ProD 1- 4** and Figure 4.10 for paracetamol **ProD 2**, **ProD 3.** As shown in the figures, excellent linearity with correlation coefficient (R^2) of 0.995, 0.970, 0.995 and 0.982 for tranexamic acid **ProD 1-4** respectively, and the (R^2) was 0.995 for paracetamol **ProD 2** and **ProD 3** was obtained.

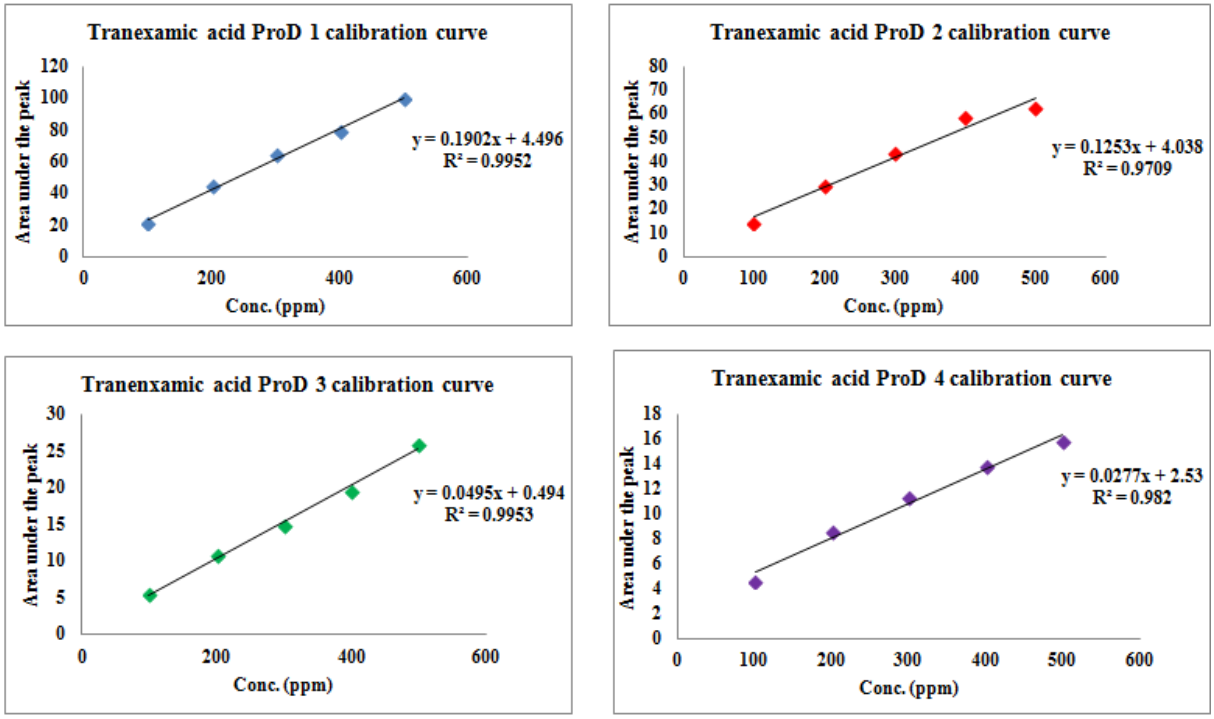

Figure 4.9. Calibration curves for tranexamic acid **ProD 1-4**.

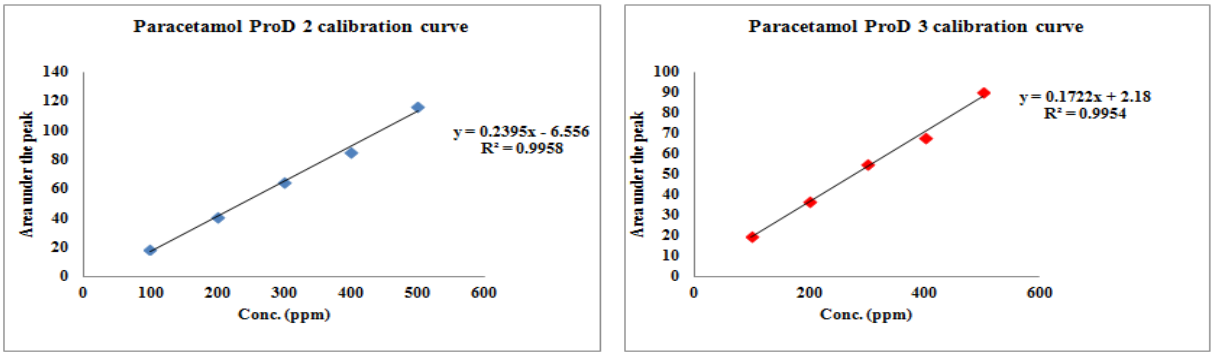

Figure 4.10. Calibration curves for paracetamol **ProD 2** and **ProD 3**.

4.3.Hydrolysis studies

4.3.1. Tranexamic acid ProD 1-4:

The kinetics of the acid-catalyzed hydrolysis studies were carried out in aqueous buffer in the same manner as that done by Kirby on Kirby's enzyme model **1-9** [73]. This is in order to explore whether the prodrug hydrolyzes in aqueous medium and to what extent, suggesting the fate of the prodrug in the system. Acid-catalyzed hydrolysis kinetics of the synthesized tranexamic acid **ProD 1-4** were studied in four different aqueous media, 1N HCl, buffer pH 2, buffer pH 5 and buffer pH 7.4. Under the experimental conditions, the target compounds hydrolyzed to release the parent drug as evident by HPLC analysis. At constant pH and temperature, the reaction displayed strict first order kinetics as the *k*obs was fairly constant and a straight plot was obtained on plotting log concentration of residual prodrug vs. time. The rate constant (*k*obs) and the corresponding half-lives ($t_{1/2}$) for tranexamic acid prodrug **ProD 1-4** in the different media were calculated from the linear regression equation correlating the log concentration of the residual prodrug vs. time. The 1N HCl and pH 2 were selected to examine the intra-conversion of the tranexamic acid prodrug in pH as of stomach, because the mean fasting stomach pH of adult is approximately 1-2. In addition, buffer pH 5 mimics the beginning small intestine pathway. pH 7.4 was selected to examine the intra-conversion of the tested prodrug in blood circulation system. Acid-catalyzed hydrolysis of the tranexamic acid **ProD 1** was found to be higher at 1N HCl than at pH 2 and 5 (Figures 4.11, 4.12, 4.13 and 4.14). At 1N HCl, the prodrug was hydrolyzed to release the parent drug in less than one hour. On the other hand, at pH 7.4, the prodrug was entirely stable and no release of the parent

drug was observed. Since the pK_a of tranexamic acid **ProD 1** is in the range of 3-4, it is expected that at pH 5 the anionic form of the prodrug will be dominant and the percentage of the free acid form that undergoes the acid-catalyzed hydrolysis will be relatively low. At 1N HCl and pH 2, most of the prodrug will exist as the free acid form and at pH 7.4 most of the prodrug will be in the anionic form. Thus the discrepancy in rates at the different pH buffers. The kinetic data are listed in Table 4.1. Acid catalyzed hydrolysis of tranexamic acid **ProD 2** was found to be readily intraconverted at 1N HCl and pH 2, while it was stable at pH 5 and 7.4; according to structural feature of 2,3-dimethyl maleic moiety it contains two methyl groups on the C-C double bond (strained system) which results in a decrease of the distance between the two reactive centers (hydroxyl oxygen of the carboxylic group and the amide carbonyl carbon). Hence, the hydrolysis in 1N HCl and pH 2 of tranexamic acid **ProD 2** is faster than that of tranexamic acid **ProD 1**, Table 4.2 summarize the kinetic data for tranexamic acid **ProD 2**.

In the case of tranexamic acid **ProD 3** and **ProD 4** the interatomic distance between the neucleophile (OH) and electrophile (C=O) is too high to make the nucleophile attack accessible. Hence, no reaction was observed with these two prodrugs (Table 4.3 and 4.4).

Table 4.1: The observed *k* value and $t_{1/2}$ for the intraconverion of tranexamic acid **ProD 1** in 1N HCl and at pH 2, pH 5 and pH 7.4.

Medium	k_{obs} **(h^{-1})**	$t_{½}$ **(h)**
1N HCl	5.13×10^{-3}	0.9
Buffer pH 2	3.92×10^{-5}	23.9
Buffer pH 5	3.92×10^{-6}	270
Buffer pH 7.4	No reaction	No reaction

Table 4.2: The observed *k* value and $t_{1/2}$ for the intraconverion of tranexamic acid **ProD 2** in 1N HCl and at pH 2, pH 5 and pH 7.4.

Medium	k_{obs} **(h^{-1})**	$t_{½}$ **(h)**
1N HCl	Readily released	Readily released
Buffer pH 2	Readily released	Readily released
Buffer pH 5	No reaction	No reaction
Buffer pH 7.4	No reaction	No reaction

Table 4.3: The observed *k* value and $t_{1/2}$ for the intraconverion of tranexamic acid **ProD 3** in 1N HCl and at pH 2, pH 5 and pH 7.4.

Medium	k_{obs} **(h^{-1})**	$t_{½}$ **(h)**
1N HCl	No reaction	No reaction
Buffer pH 2	No reaction	No reaction
Buffer pH 5	No reaction	No reaction
Buffer pH 7.4	No reaction	No reaction

Table 4.4: The observed *k* value and $t_{1/2}$ for the intraconverion of tranexamic acid **ProD 4** in 1N HCl and at pH 2, pH 5 and pH 7.4.

Medium	k_{obs} **(h^{-1})**	$t_{½}$ **(h)**
1N HCl	No reaction	No reaction
Buffer pH 2	No reaction	No reaction
Buffer pH 5	No reaction	No reaction
Buffer pH 7.4	No reaction	No reaction

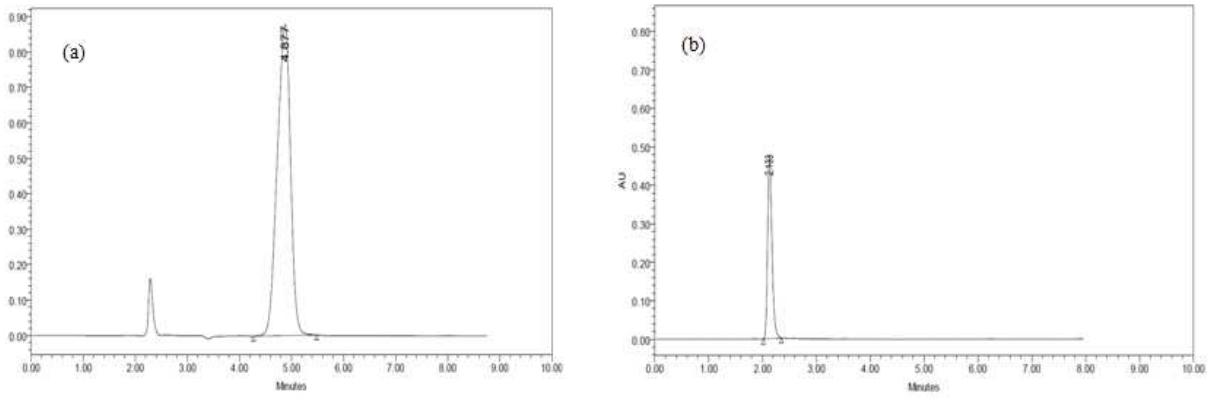

Figure 4.11. Chromatograms showing the intra-conversion of tranexamic acid **ProD 1** in 1N HCl (a) at zero time, (b) at the end of reaction**.**

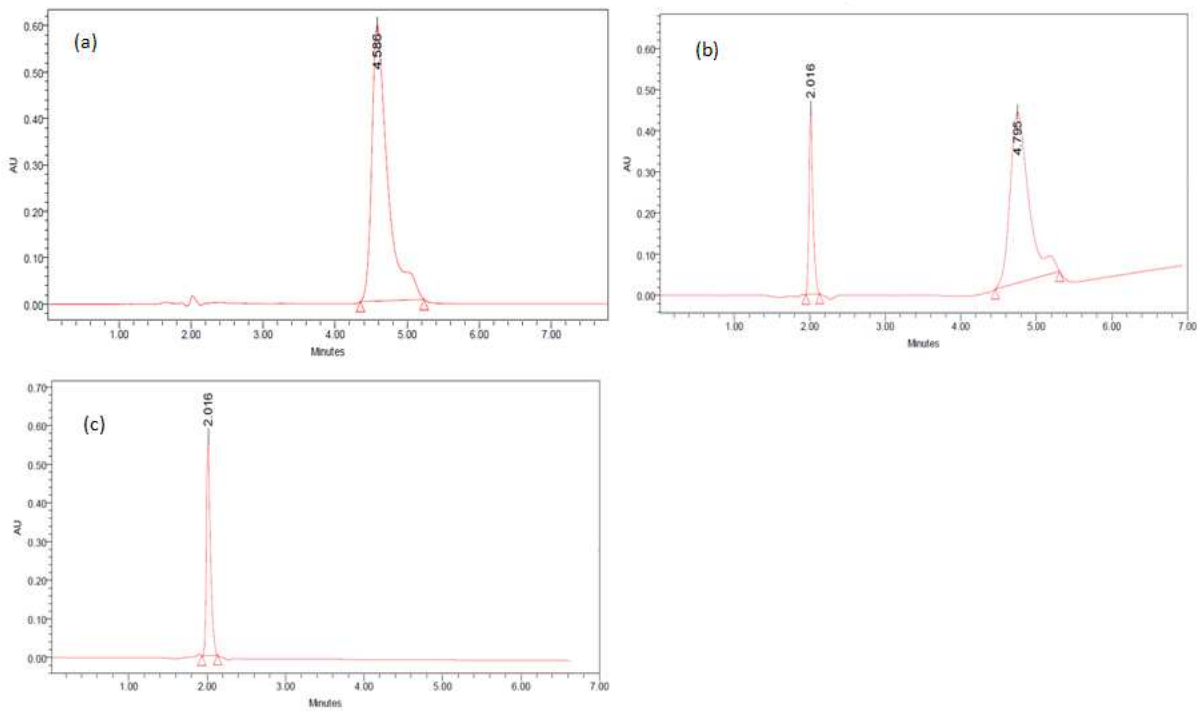

Figure 4.12. Chromatograms showing the intra-conversion of tranexamic acid **ProD 1** at pH 2 (a) at zero time, (b) after 24 hours, (c) at the end of reaction**.**

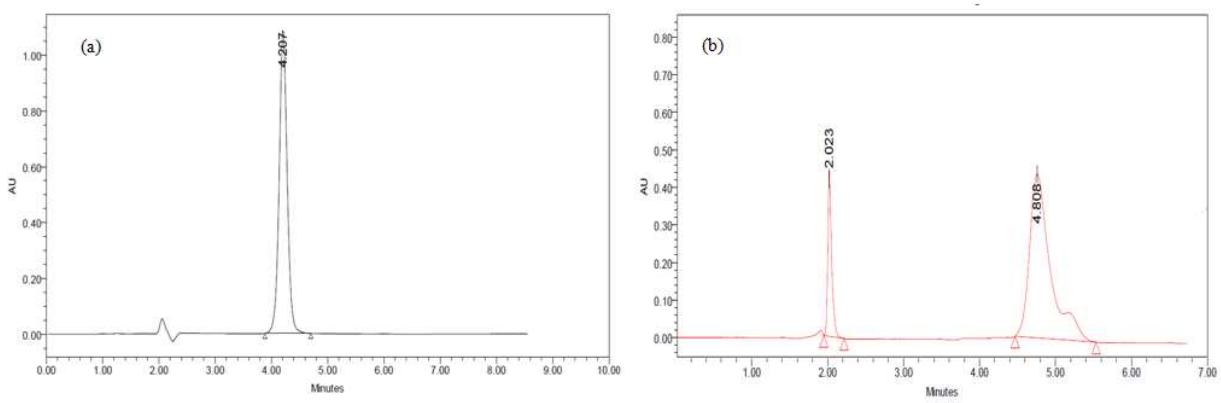

Figure 4.13. Chromatograms showing the intra-conversion of tranexamic acid **ProD 1** at pH 5 (a) at zero time, (b) after 250 hours**.**

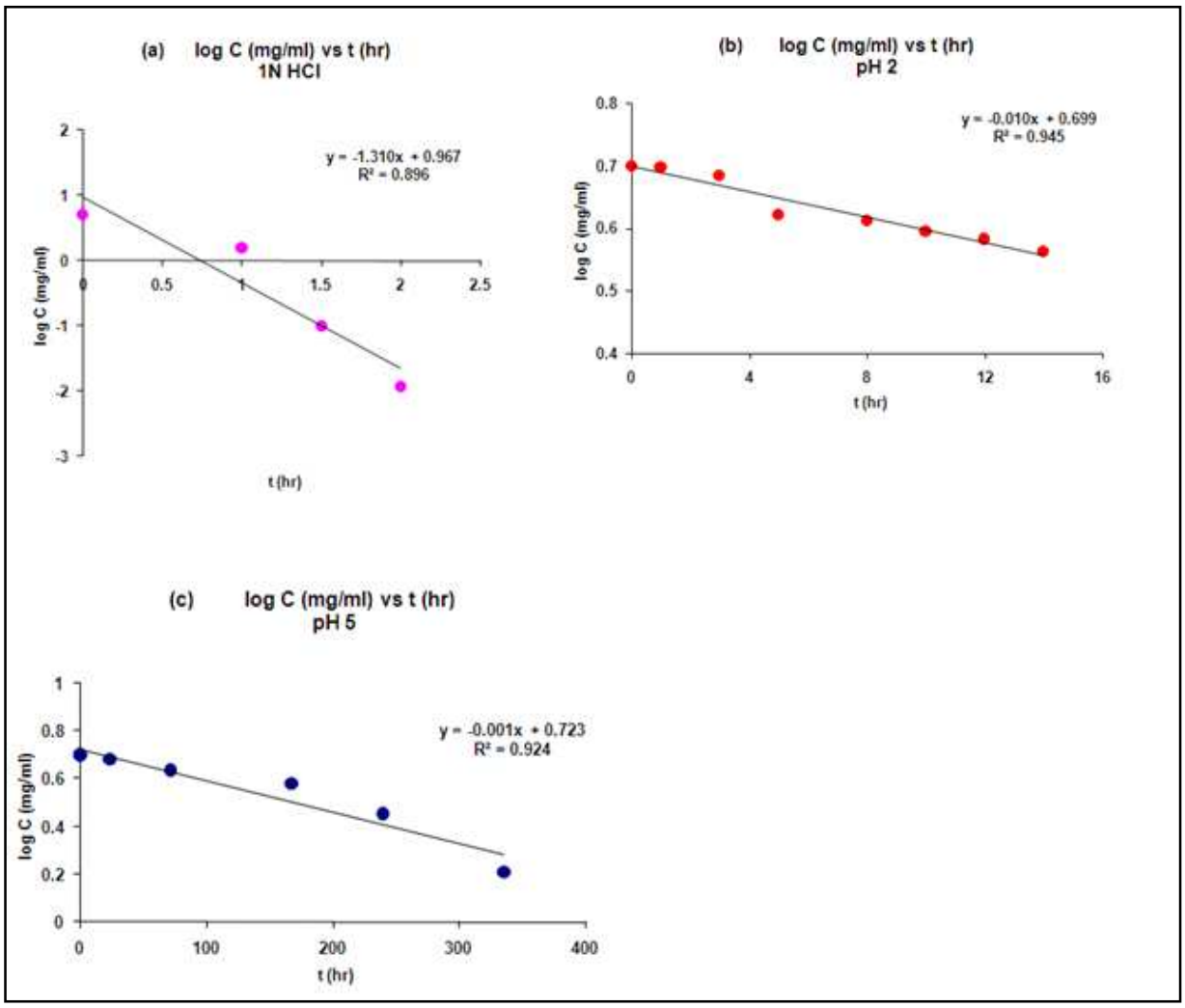

Figure 4.14. First order hydrolysis plot for the intraconverion of tranexamic acid **ProD 1** in (a) 1N HCl, (b) buffer pH 2 and (c) buffer pH 5.

4.3.2. Paracetmol ProD 2 and ProD 3

The hydrolysis reactions of paracetamol **ProD 2** and **ProD 3** were studied in three different media; 1N HCl, buffer pH 3 and buffer pH 7.4. The prodrug hydrolysis was monitored using HPLC analysis (Figures 4.15 and 4.16). At constant pH and temperature the release of paracetamol from its prodrugs was followed and showed a first order kinetics. k_{obs} (h^{-1}) and $t_{1/2}$ values for the intra-conversion of paracetamol **ProD 2** and **ProD 3** were calculated from regression equation obtained from plotting log concentration of residual of paracetamol **ProD 2 or ProD 3** vs. time (Figures 4.17 and 4.18). The kinetics results for paracetamol **ProD 2** and paracetamol **ProD 3** in the different media are summarized in Tables 4.5 and 4.6.

As shown in Tables 5 and 6 the hydrolysis rate of paracetamol **ProD 2** and paracetamol **ProD 3** at pH 7.4 was the fastest among all media, followed by the medium of pH 3. In 1N HCl no conversion of the prodrug to the parent dug was observed.

Table 4.5: The observed *k* value and $t_{1/2}$ for the intra-conversion of paracetamol **ProD 2** in 1N HCl and buffers pH 3 and 7.4.

Medium	k_{obs} **(h^{-1})**	$t_{½}$ **(h)**
1N HCl	No reaction	No reaction
Buffer pH 3	6.3×10^{-5}	3
Buffer pH 7.4	6.1×10^{-4}	0.3

Table 4.6: The observed *k* value and $t_{1/2}$ for the intra-conversion of paracetamol **ProD 3** in 1N HCl and buffers pH 3 and 7.4.

Medium	k_{obs} **(h^{-1})**	$t_{½}$ **(h)**
1N HCl	No reaction	No reaction
Buffer pH 3	7.5×10^{-6}	27
Buffer pH 7.4	9.02×10^{-5}	12

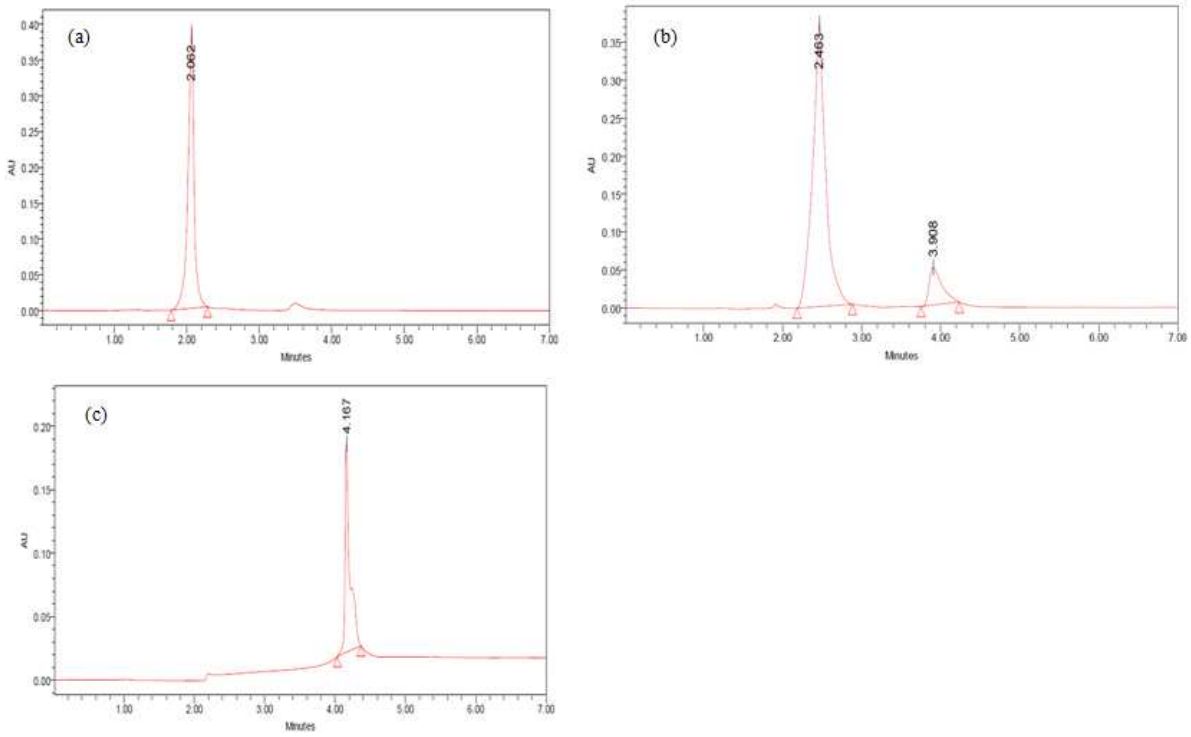

Figure 4.15. Chromatograms showing the intra-conversion of paracetamol **ProD 3** at pH 3 (a) at zero time, (b) after 4 hours, (c) at the end of reaction**.**

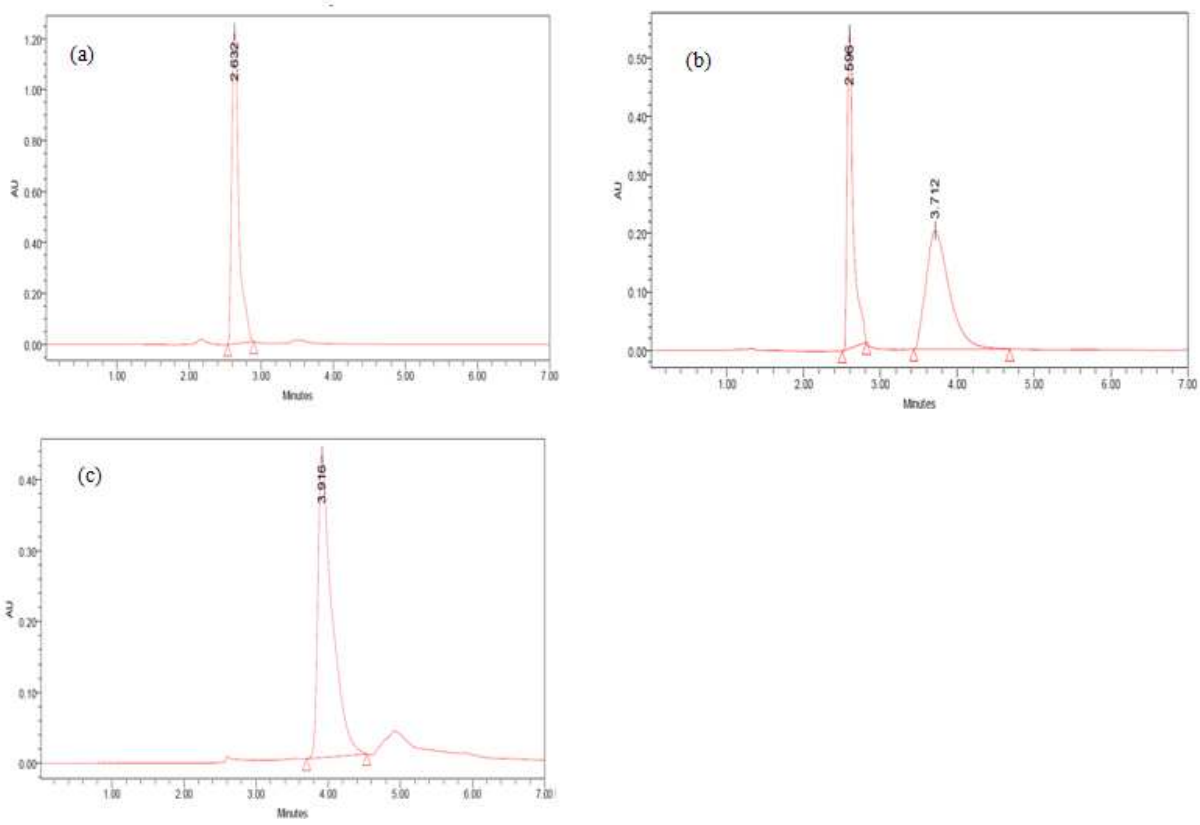

Figure 4.16. Chromatograms showing the intra-conversion of paracetamol **ProD 3** at pH 7.4 (a) at zero time, (b) after 4 hours, (c) at the end of reaction**.**

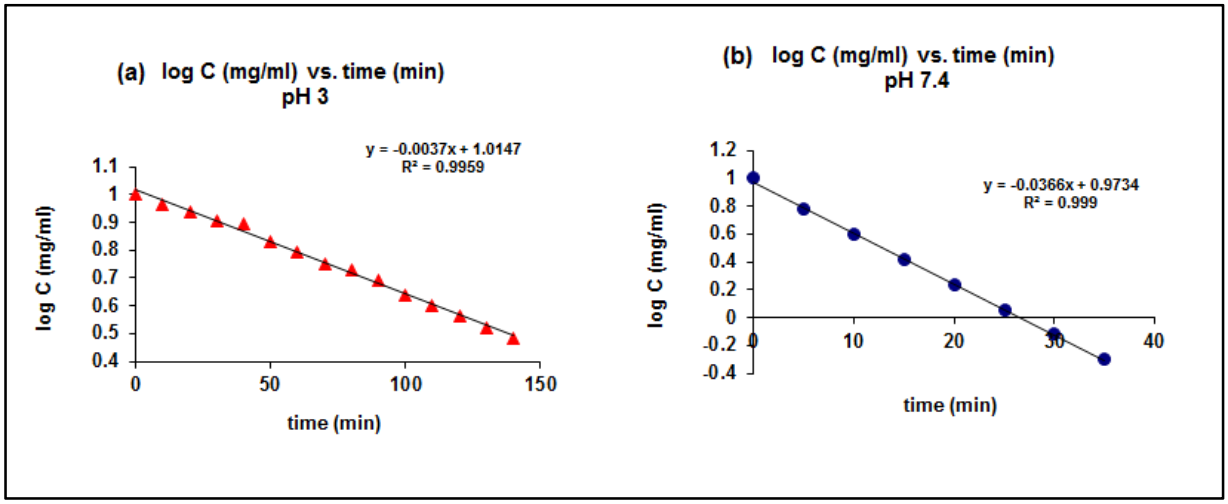

Figure 4.17. First order hydrolysis plot for paracetamol **ProD 2** in (a) buffer pH 3 and (b) buffer pH 7.4.

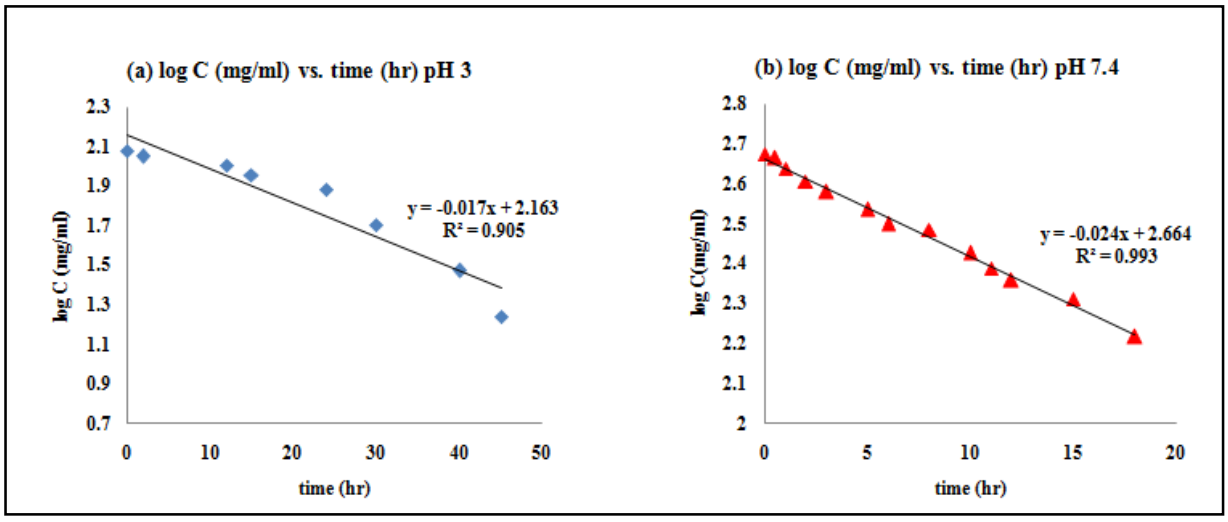

Figure 4.18. First order hydrolysis plot for paracetamol **ProD 3** in (a) buffer pH 3 and (b) buffer pH 7.4.

At pH 7.4 paracetamol **ProD 2** and **ProD 3** are mainly exist as carboxylate anion forms that are expected to undergo fast hydrolysis according to Bruice's mechanism shown in Figure 2.5 [72]. At pH 3, the prodrugs exist in both forms, the anion and the free carboxylic acid forms due to the fact that the pKa of the prodrugs is around 3. In 1N HCl, the prodrugs are entirely exist as the carboxylic free acid form and since only the

carboxylate anion form undergoes Bruice's cyclization the hydrolysis rate in 1N HCl is almost negligible or zero.

In vitro binding for paracetamol **ProD 2** to bitter taste receptors was tested in Germany and the result revealed that this prodrug lacks any binding affinity and it was found not to have any bitter sensation.

Conclusions and Future directions

Chapter Five

5. Conclusions and Future directions

5.1. Conclusions:

Based on Kirby`s enzyme model (Proton transfer in N-alkylmaleamic acids) four different tranexamic acid prodrugs were synthesized and their acid-catalyzed hydrolysis demonstrated that the rate-limiting step was the collapse of the tetrahedral intermediate. The experimental $t_{1/2}$ value for tranexamic acid **ProD 1** in 1N HCl, buffer pH 2 and buffer pH 5 were 54 minutes, 23.9 hours and 270 hours, respectively. On the other hand, no hydrolysis was observed at pH 7.4. The lack of the hydrolysis at pH 7.4 might be due to the fact that at this pH tranexamic acid **ProD 1** exists mainly in the ionized form (pK_a about 4) taking into consideration that the free acid form is a mandatory requirement for the acid-catalyzed hydrolysis to proceed. Tranexamic acid **ProD 2** was readily converted in 1 N HCl and pH 2 while it was stable at pH 5 and pH 7.4. Tranexamic acid **ProD 3** and **Prod 4** were stable in 1 N HCl, pH 2, pH 5 and pH 7.4 and no reaction was observed. This may be due to the long interatomic distance between the nucleophile (OH) and electrophile (C=O) which renders any nucleophile attack. Hence additional tranexamic acid prodrugs with reasonable intra-conversion rate at pH 6.5 and pH 7.4 can be synthesized

Bruice's enzyme model was used to design, synthesize three different bitterless paracetamol prodrugs. In vitro kinetic study of paracetamol **ProD 2** and **ProD 3** was performed in 1 N HCl, pH 3 and pH 7.4. Both prodrugs were stable in 1N HCl, whereas, they intraconverted to release their parent drug (paracetamol) in pH 3 and pH 7.4. The experimental $t_{1/2}$ values for Paracetamol **ProD 2** in pH 3 and pH 7.4 were 3 hours and 18 minutes respectively, while that for paracetamol **ProD 3** in pH 3 and pH 7.4 were 27 hours and 12 hours, respectively. In vitro biding for paracetamol **ProD 2** to bitter taste receptors revealed that this prodrug lacks any binding affinity and it was found not to have any bitter sensation. This suggests, that paracetamol **ProD 2** can replace its parent drug, paracetamol, for the use as bitterless antipyretic drug for geriatrics and pediatrics

5.2. Future directions:

Synthesis of additional tranexamic acid prodrugs that may be intra-converted to their parent drug, tranexamic acid, at pH 6.5 (intestine) and pH 7.4 (blood circulation system). In vivo pharmacokinetic studies will be done in order to determine the bioavailability and the duration of action of the tested prodrugs.

In vivo pharmacokinetic studies for paracetamol **ProD 2** and in vitro binding for paracetamol **ProD 3** to bitter taste receptors will be done.

References

References

1. Albert, A. (1958). Chemical aspects of selective toxicity. *Nature*, *182*(4633), 421.
2. Huttunen, K. M., Raunio, H., & Rautio, J. (2011). Prodrugs—from serendipity to rational design. *Pharmacological reviews*, *63*(3), 750-771.
3. Stella, V. J. (2010). Prodrugs: Some thoughts and current issues. *Journal of pharmaceutical sciences*, *99*(12), 4755-4765.
4. Wu, K. M. (2009). A new classification of prodrugs: regulatory perspectives.*Pharmaceuticals*, *2*(3), 77-81.
5. Remington, J. P. (2006). *Remington: The science and practice of pharmacy* (Vol. 1). D. B. Troy & P. Beringer (Eds.). Wolters Kluwer Health.
6. Karaman, R. (2013). Prodrug Design vs. Drug Design. *Drug Des*, *2*, e114.
7. Fleisher, D., Bong, R., & Stewart, B. H. (1996). Improved oral drug delivery: solubility limitations overcome by the use of prodrugs. *Advanced Drug Delivery Reviews*, *19*(2), 115-130.
8. Müller, C. E. (2009). Prodrug approaches for enhancing the bioavailability of drugs with low solubility. *Chemistry & biodiversity*, *6*(11), 2071-2083.
9. Stella, V. J., & Nti-Addae, K. W. (2007). Prodrug strategies to overcome poor water solubility. *Advanced drug delivery reviews*, *59*(7), 677-694.
10. Liederer, B. M., & Borchardt, R. T. (2006). Enzymes involved in the bioconversion of ester-based prodrugs. *Journal of pharmaceutical sciences*, *95*(6), 1177-1195.
11. Tegeli, V. S., Thorat, Y. S., Chougule, G. K., Shivsharan, U. S., Gajeli, G. B., & Kumbhar, S. T. (2010). Review on Concepts and Advances in Prodrug Technology. *International Journal*, *1*.
12. Karaman, R. (2012). Computationally Designed Enzyme Models to Replace Natural Enzymes in Prodrug Approaches. *Drug Des*, *1*, e111.
13. Karaman, R. (2013) Prodrug Design by Computation Methods: A New Era. *Drug Des*, *1*, e113.

14. Williams-Johnson, J. A., McDonald, A. H., Strachan, G. G., & Williams, E. W. (2010). Effects of tranexamic acid on death, vascular occlusive events, and blood transfusion in trauma patients with significant haemorrhage (CRASH-2): a randomised, placebo-controlled trial. *West Indian Medical Journal*, *59*(6), 612-624.
15. Mayur, G., Purvi, P., Ashoo, G., & Pankaj, D. (2007). Efficacy of tranexamic acid in decreasing blood loss during and after cesarean section: a randomized case controlled prospective study. *J Obstet Gynecol India*, *57*(3), 227-230.
16. Liumbruno, G. M., Bennardello, F., Lattanzio, A., Piccoli, P., & Rossetti, G. (2011). Recommendations for the transfusion management of patients in the peri-operative period. II. The intra-operative period. *Blood Transfusion*, *9*(2), 189.
17. Lukes, A. S., Kouides, P. A., & Moore, K. A. (2011). Tranexamic acid: a novel oral formulation for the treatment of heavy menstrual bleeding. *Women's Health*,*7*(2), 151-158.
18. Lukes, A. S., Moore, K. A., Muse, K. N., Gersten, J. K., Hecht, B. R., Edlund, M., & Shangold, G. A. (2010). Tranexamic acid treatment for heavy menstrual bleeding: a randomized controlled trial. *Obstetrics & Gynecology*, *116*(4), 865-875.
19. Cardone, D., & Klein, A. A. (2009). Perioperative blood conservation. *European Journal of Anaesthesiology (EJA)*, *26*(9), 722-729.
20. Nilsson, I. M. (1980). Clinical pharmacology of aminocaproic and tranexamic acids. *Journal of Clinical Pathology*, *33*(Suppl 14), 41-47.
21. AlAmeel, T., & West, M. (2011). Tranexamic acid treatment of life-threatening hematuria in polycystic kidney disease. *International journal of nephrology*, *2011*.
22. Wu, S. F., Shi, H. Y., & Chen, Y. (2008). Treatment of melasma with oral administration of tranexamic acid. *Chinese Journal of Aesthetic and Plastic Surgery*, *2*, 010.
23. Graham, G. G., & Scott, K. F. (2005). Mechanism of action of paracetamol. *American journal of therapeutics*, *12*(1), 46-55.
24. Hoftiezer, J. W., O'Laughlin, J. C., & Ivey, K. J. (1982). Effects of 24 hours of aspirin, Bufferin, paracetamol and placebo on normal human gastroduodenal mucosa. *Gut*, *23*(8), 692-697.

25. Reilly, J.W. (2002). Pharmaceutical necessities in Remington. *The science and practice of pharmacy*, Mack Publishing company, 1018-1020
26. Behrens, M., Reichling, C., Batram, C., Brockhoff, A., & Meyerhof, W. (2009). Bitter taste receptors and their cells. *Annals of the New York Academy of Sciences*, *1170*(1), 111-115.
27. Schiffman, H.S. (2000). Sensation and Perception. *An Integrated Approach*. 5th ed, 163-169.
28. Pilbrant, Å., Schannong, M., & Vessman, J. (1981). Pharmacokinetics and bioavailability of tranexamic acid. *European journal of clinical pharmacology*, *20*(1), 65-72.
29. Hejaz, H., Karaman, R., & Khamis, M. (2012). Computer-assisted design for paracetamol masking bitter taste prodrugs. *Journal of molecular modeling*, *18*(1), 103-114.
30. Milstien, S., & Cohen, L. A. (1970). Concurrent general-acid and general-base catalysis of esterification. *Journal of the American Chemical Society*, *92*(14), 4377-4382.
31. Bruice, T. C., & Pandit, U. K. (1960). The effect of geminal substitution ring size and rotamer distribution on the intramolecular nucleophilic catalysis of the hydrolysis of monophenyl esters of dibasic acids and the solvolysis of the intermediate anhydrides. *Journal of the American Chemical Society*, *82*(22), 5858-5865.
32. Bruice, T. C., & Pandit, U. K. (1960). INTRAMOLECULAR MODELS DEPICTING THE KINETIC IMPORTANCE OF „FIT" IN ENZYMATIC CATALYSIS. *Proceedings of the National Academy of Sciences of the United States of America*, *46*(4), 402.
33. Greenwald, R. B., Choe, Y. H., Conover, C. D., Shum, K., Wu, D., & Royzen, M. (2000). Drug delivery systems based on trimethyl lock lactonization: poly (ethylene glycol) prodrugs of amino-containing compounds. *Journal of medicinal chemistry*, *43*(3), 475-487.
34. Reddy, M. R., & Erion, M. D. (Eds.). (2001). *Free energy calculations in rational drug design*. Springer.

35. Dewar, M. J., & Thiel, W. (1977). Ground states of molecules. 38. The MNDO method. Approximations and parameters. *Journal of the American Chemical Society*, *99*(15), 4899-4907.
36. Bingham, R. C., Dewar, M. J., & Lo, D. H. (1975). Ground states of molecules. XXV. MINDO/3. Improved version of the MINDO semiempirical SCF-MO method.*Journal of the American Chemical Society*, *97*(6), 1285-1293.
37. Parr, R. G., & Yang, W. (1989). *Density-functional theory of atoms and molecules* (Vol. 16). Oxford university press.
38. Karaman, R. (2008). Analysis of Menger's 'spatiotemporal hypothesis'.*Tetrahedron Letters*, *49*(41), 5998-6002.
39. Karaman, R. (2009). A new mathematical equation relating activation energy to bond angle and distance: a key for understanding the role of acceleration in lactonization of the trimethyl lock system. *Bioorganic chemistry*, *37*(1), 11-25.
40. Karaman, R. (2009). Accelerations in the lactonization of trimethyl lock systems are due to proximity orientation and not to strain effects. *Organic Chemistry International*, *2009*.
41. Karaman, R. (2009). The effective molarity (EM) puzzle in proton transfer reactions. *Bioorganic chemistry*, *37*(4), 106-110.
42. Karaman, R. (2009). Cleavage of Menger's aliphatic amide: a model for peptidase enzyme solely explained by proximity orientation in intramolecular proton transfer. *Journal of Molecular Structure: THEOCHEM*, *910*(1), 27-33.
43. Karaman, R. (2009). The gem-disubstituent effect—a computational study that exposes the relevance of existing theoretical models. *Tetrahedron Letters*, *50*(44), 6083-6087.
44. Karaman, R. (2009). Analyzing Kirby's amine olefin—a model for amino acid ammonia lyases. *Tetrahedron Letters*, *50*(52), 7304-7309.
45. Karaman, R. (2010). Effects of substitution on the effective molarity (EM) for five membered ring-closure reactions–A computational approach. *Journal of Molecular Structure: THEOCHEM*, *939*(1), 69-74.

46. Karaman, R. (2010). The effective molarity (EM) puzzle in intramolecular ring-closing reactions. *Journal of Molecular Structure: THEOCHEM*, *940*(1), 70-75.
47. Karaman, R. (2010). The efficiency of proton transfer in Kirby's enzyme model, a computational approach. *Tetrahedron Letters*, *51*(16), 2130-2135.
48. Karaman, R. (2010). Proximity vs. strain in intramolecular ring-closing reactions. *Molecular Physics*, *108*(13), 1723-1730.
49. Karaman, R. (2010). The effective molarity (EM)–a computational approach.*Bioorganic chemistry*, *38*(4), 165-172.
50. Karaman, R. (2010). A general equation correlating intramolecular rates with 'attack'parameters: distance and angle. *Tetrahedron Letters*, *51*(39), 5185-5190.
51. Karaman, R. (2010). Prodrugs of aza nucleosides based on proton transfer reaction. *Journal of computer-aided molecular design*, *24*(12), 961-970.
52. Karaman, R. (2013). Prodrugs for masking bitter taste of antibacterial drugs—a computational approach. *Journal of molecular modeling*, 1-14.
53. Karaman, R., & Alfalah, S. (2010). Multi Transition States for SN2 Reaction in Intramolecular Processes.
54. Karaman, R., Amly, W., Scrano, L., Mecca, G., & Bufo, S. A. (2013). Computationally designed prodrugs of statins based on Kirby's enzyme model.*Journal of molecular modeling*, *19*(9), 3969-3982.
55. Karaman, R., Fattash, B., & Qtait, A. (2013). The future of prodrugs-design by quantum mechanics methods. *Expert opinion on drug delivery*, *10*(5), 713-729.
56. Karaman, R., & Pascal, R. (2010). A computational analysis of intramolecularity in proton transfer reactions. *Org. Biomol. Chem.*, *8*(22), 5174-5178.
57. Milstien, S., & Cohen, L. A. (1970). Rate acceleration by stereopopulation control: models for enzyme action. *Proceedings of the National Academy of Sciences*, *67*(3), 1143-1147.
58. Milstien, S., & Cohen, L. A. (1972). Stereopopulation control. I. Rate enhancement in the lactonizations of o-hydroxyhydrocinnamic acids. *Journal of the American Chemical Society*, *94*(26), 9158-9165.

59. Menger, F. M. (1983). Directionality of organic reactions in solution.*Tetrahedron*, *39*(7), 1013-1040.
60. Menger, F. M. (1985). On the source of intramolecular and enzymatic reactivity.*Accounts of chemical Research*, *18*(5), 128-134.
61. Menger, F. M. (2005). An alternative view of enzyme catalysis. *Pure and applied chemistry*, *77*(11), 1873-1886.
62. Menger, F. M., Chow, J. F., Kaiserman, H., & Vasquez, P. C. (1983). Directionality of proton transfer in solution. Three systems of known angularity.*Journal of the American Chemical Society*, *105*(15), 4996-5002.
63. Menger, F. M., Galloway, A. L., & Musaev, D. G. (2003). Relationship between rate and distance. *Chemical Communications*, (18), 2370-2371.
64. Menger, F. and M. Ladika, *Fast hydrolysis of an aliphatic amide at neutral pH and ambient temperature. A peptidase model.* Journal of the American Chemical Society, 1988. **110**(20): p. 6794-6796.
65. Menger, F. M., & Ladika, M. (1990). Remote enzyme-coupled amine release.*The Journal of Organic Chemistry*, *55*(10), 3006-3007.
66. Brown, R., & Van Gulick, N. (1956). Notes-The Geminal Alkyl Effect on the Rates of Ring Closure of Bromobutylamines. *The Journal of Organic Chemistry*,*21*(9), 1046-1049.
67. Kirby, A. J. (1980). Effective molarities for intramolecular reactions. *Adv. Phys. Org. Chem*, *17*, 183-278.
68. Kirby, A. J. (1996). Enzyme mechanisms, models, and mimics. *Angewandte Chemie International Edition in English*, *35*(7), 706-724.
69. Kirby, A. J., Lima, M. F., da Silva, D., Roussev, C. D., & Nome, F. (2006). Efficient intramolecular general acid catalysis of nucleophilic attack on a phosphodiester. *Journal of the American Chemical Society*, *128*(51), 16944-16952.
70. Kirby, A. J., & Williams, N. H. (1991). Efficient intramolecular general acid catalysis of vinyl ether hydrolysis by the neighbouring carboxylic acid group. *J. Chem. Soc., Chem. Commun.*, (22), 1643-1644.

71. Kirby, A. J., & Williams, N. H. (1994). Efficient intramolecular general acid catalysis of enol ether hydrolysis. Hydrogen-bonding stabilisation of the transition state for proton transfer to carbon. *J. Chem. Soc., Perkin Trans. 2*, (4), 643-648.
72. Karaman, R. (2009). Reevaluation of Bruice's proximity orientation. *Tetrahedron Letters*, *50*(4), 452-456.
73. Kirby, A. J., & Williams, N. H. (1994). Efficient intramolecular general acid catalysis of enol ether hydrolysis. Hydrogen-bonding stabilisation of the transition state for proton transfer to carbon. *J. Chem. Soc., Perkin Trans. 2*, (4), 643-648.
74. Houk, K. N., Tucker, J. A., & Dorigo, A. E. (1990). Quantitative modeling of proximity effects on organic reactivity. *Accounts of Chemical Research*, *23*(4), 107-113.

الخلاصة

Prodrug هو مادة كيميائية يتم فيها ربط العقار تساهميا إلى مجموعة كيميائية ، بحيث تؤثر هذه المجموعة المرتبطة مؤقتا على الخصائص الفيزيائية للدواء لزيادة الفائدة أو تقليل سميتها. يجب أن يتم تحويل الProdrug إلى شكله النشط من قبل الأيض و / أو العمليات الكيميائية داخل الجسم، من الممكن ان تتم عملية التحويل بالإعتماد على عملية التمثيل الغذائي أو باستخدام الانزيمات التي وزعت في جميع أنحاء الجسم. هذه الإنزيمات قد تقلل إما التوافر الحيوي للدواء ، أو قد تظهرمشكلة تعدد الأشكال الوراثية مما يؤدي إلى التباين في تفعيل الProdrug ، وبالتالي تؤثرعلى فعالية وسلامة الدواء المساعد. في العقود القليلة الماضية استخدمت أساليب الكيمياء الحسابية في حساب الخصائص الفيزيائية و الجزيئية للمركبات. باستخدام هذه الأداة من الممكن تصميمProdrug بحيث يتحول الProdrug الى الدواء النشط عن طريق روابط داخل الجزيء نفسه دون أي تدخل من الإنزيمات. بناء على حسابات DFT تم تصميم اربع Prodrugs ل حمض الترانيكساميك وثلاثة للباراسيتامول، ومن ثم تمت دراسة تحويل هذه الأدوية إلى الدواء الأصلي ووجد ان $t_{1/2}$ تتأثر إلى حد كبير بدرجة حموضة الوسط. ل **ProD 1** tranexamic acid كانت النتائج التجريبية لل $t_{1/2}$ في حمض الهيدروكلوريد، درجة حموضة 2 و درجة حموضة 5 كالتالي 54 دقيقة، 23.9 ساعة و 270 ساعة، على التوالي.**ProD 2** Tranexamic acid تم تحويله بسرعه في حمض الهيدروكلوريد، درجة حموضة 2 بينما كان مستقر تماما في درجة الحموضة 5 و 7.4. من ناحية أخرى ، **ProD 3** and **ProD 4** tranexamic acid لم يكن هناك اي تحول للدواء النشط على جميع درجات الحموضة المستخدمه في هذه الدراسة. كانت $t_{1/2}$ التجريبية ل paracetamol **ProD 2** في درجة الحموضة 7.4 و 3، 3 ساعات و 18 دقيقة على التوالي أما ل paracetamol **ProD 3** كانت 27 ساعة في درجة الحموضة 3 و 12 ساعة في درجة الحموضة 7.4. تم فحص paracetamol **ProD 2** في المختبر المتخصص لمستقبلات الطعم المر وكشفت النتائج أن هذا ال Prodrug يفتقر إلى أي إحساس بالطعم المر. هذا يشير إلى أن paracetamol **ProD 2** يمكن أن تحل محل، الباراسيتامول ، ويتم استخدامه كخافض للحرارة للمسنين و الأطفال.

عمادة الدراسات العليا

جامعة القدس

تصنيع ودراسة المواصفات ل الأدوية المساعده المصممة ل حمض ترانزاميك و براسيتامول

اعداد

هبه نعيم خميس غريب

رسالة ماجستير

فلسطين ـ القدس

1435هـ / م 2014

تصنيع ودراسة المواصفات ل الأدوية المساعده المصممة ل حمض ترانزاميك و براسيتامول

إعداد

هبه نعيم خميس غريب

بكالوريوس صيدلة- جامعة القدس، فلسطين.

المشرف الرئيسي: بروفيسور رفيق قرمان

قدمت هذه الأطروحة استكمالا لمتطلبات درجة الماجستير في العلوم الصيدلانية من كلية الدراسات العليا جامعة القدس-فلسطين.

1435 هـ / م 2014